# The Final Progress Report

**Grant/Cooperative Agreement Number: PAR12-252/ OH010473-02**

**PROGRAM DIRECTOR / PRINCIPAL INVESTIGATOR**

Xiaozhong Yu

**Affiliation**

Environmental Health Science Building
150 East Green Street
Athens, GA 30602
E-MAIL ADDRESS: yuxz@uga.edu

**TITLE OF PROJECT**

A 3D Mini-Testis Model for Reproductive Toxicity Testing

**APPLICANT ORGANIZATION**

The University of Georgia Research Foundation, Inc.
200 D. W. Brooks Drive
617 Boyd GSRC
Athens, GA 30602
Tel: 706-542-3545
Fax: 706-542-7472
DUNS: 0043155784

**Grant/Cooperative Agreement Project Period: 9/1/2013 – 8/31/2016**

**The date the final report was completed: 11-23-16**

**Abstract (486 words)**

Occupational exposure to reproductive toxicants occurs via inhalation, skin absorption, or ingestion. Thousands of chemicals exist in the workplace; there is limited or no toxicological information including reproductive and developmental (R/D) toxicity available for many industrial chemicals. Toxicity testing on animals represents one of the largest uses of animals yet it also has been an extraordinarily challenging area in which to implement *in vitro* alternatives. Since the report “Toxicity Testing in the 21st Century” by the National Research Council (NRC, 2007) envisioned that *in vivo* animal testing can eventually be replaced by a combination of *in silico* and *in vitro* approaches, the demand to identify *in vitro* models for R/D toxicity has grown. In this proposal, we established an *in vitro* “mini-testis” model from testicular cell lines, which finally eliminated the need of animals. We created a *niche* environment in which spermatogonial stem cells could be maintained and directed to proliferate and undergo meiosis and complete spermatogenesis. Based on this novel *in vitro* model, we established a toxicity-based high throughput assay. We selected 32 known reproductive toxicants and applied the high-throughput assay to compared their toxicity across multiple *in vitro cell culture* models. The comparison between the *in vitro* toxicity (IC50) and *in vivo* reproductive toxicity (lowest observed adverse effect level on the reproductive system) was conducted. We observed a strongest correlation of IC50 of the cell viability between this *in vitro* testicular co-culture model and *in vivo* testing results, but not with any single testicular cell culture models such as spermatogonia, Sertoli cell or Leydig cells. We have demonstrated that this novel *in vitro* co-culture model may be useful in screening testicular toxicants in a wide concentration range and prioritize chemicals for future experiments. Furthermore, we developed an automated multi-parametric High Content Analysis (HCA) and high throughput screening assays, representing a wide spectrum of cellular and molecular events that potentially lead to impaired male reproductive function, including nuclear morphology, DNA content, cytoskeletal integrity, cell cycle, and DNA damage responses in a dose and time-dependent manner. We applied this validated HCA approaches to characterize and compare the testicular toxicities of bisphenol A (BPA) and three selected commercially available BPA analogues: bisphenol S, bisphenol AF and tetrabromobisphenol A. Our results demonstrated that this novel *in vitro* model provides a cost-efficient screen tool for potential R/D toxicity of chemicals in the workplace, and will provide importance data for establishing exposure limit in workplace for effective prevention of R/D toxicity in workplace such as MANUFACTURING, MINING, OIL AND GAS EXTRACTION and PUBLIC SAFETY. The research conducted so far has generated 12 publications, 9 conference proceedings, and generated testicular toxicity data regarding the chemicals in workplace, and provided data for risk assessment. This funding opportunity also supported the career development of Dr. Yu in reproductive toxicology, his long-term effort in seeking and promoting *in vitro* animal alternatives. Therefore, this proposal met the mission of Cancer, Reproductive, and Cardiovascular Research Program (CRC).

*Section 1 of the Final Progress Report (2-page limit)*

**Significant (Key) Findings.**

1. **Establishment of animal-free in *vitro* three dimensional Testicular cell (3D-TCCS) model from testicular cell lines.**

*In vitro* culture systems have been used to evaluate testicular changes during normal development or treatment with chemicals. So far, these *in vitro* primary testicular cells co-culture models have their disadvantage in employing animals for the isolation of these testicular cells and the complicated isolation procedure leads to inconsistency of these primary testicular cells. As original proposed, we examined and optimized the protocol, and successfully established an animal-free *in vitro* mini-testis for the reproductive and developmental (R/D) toxicity testing. We created a *niche* environment in which spermatogonial stem cells can be maintained and directed to proliferate and undergo meiosis and complete spermatogenesis.

2. **Establishment of a toxicity-based high throughput 3D-TCCS model for R/D toxicity evaluation.**

We selected 32 known reproductive toxicants and applied toxicity-based high-throughput assay to examine their toxicity *in vitro* 3D-TCCS model. We also compared to any single cell culture model of spermatogonia, Sertoli cell or Leydig cells. The comparison between the *in vitro* toxicity (IC50 of cell viability) and *in vivo* reproductive toxicity (lowest observed adverse effect level on the reproductive system) was conducted. We observed a strongest correlation of IC50 of the cell viability between this *in vitro* testicular co-culture model and *in vivo* testing results, but not with any single testicular cell culture models. We have demonstrated that this novel *in vitro* co-culture model may be useful in screening testicular toxicants in a wide concentration range and prioritize chemicals for future experiments.

3. **Integrated pathway-based high content (HCA) and high throughput (HTP) screening assay in the 3D-TCCS model**

High-content analysis (HCA) has been demonstrated to be particularly useful for toxicity testing and prediction as it enables quantitative measurements of multiple endpoints as well as visualization of the spatial and temporal dynamic processes of cellular events. By linking chemical-biological interactions with sequential key events at multiple biological responses, adverse outcome pathways provide a mechanism-based framework to support the hazard assessment of chemicals. We developed an automated multi-parametric screening assays, representing a wide spectrum of cellular and molecular events that potentially lead to impaired male reproductive function, including nuclear morphology, DNA content, cytoskeletal integrity, cell cycle, and DNA damage responses in a dose and time-dependent manner. We applied this validated HCA approaches to characterize and compare the testicular toxicities of BPA and three selected commercially available BPA analogues: bisphenol S (BPS), bisphenol AF (BPAF) and tetrabromobisphenol A (TBBPA). Our results demonstrated that this *in vitro* model combined with HCA can be utilized for a quantitative screening of chemical effects in spermatogonial cells and enable rapid and cost-effective measurement of the multidimensional biological profile of toxicity.

4. **Comparative testicular toxicity of Bisphenol S (BPS), bisphenol AF (BPAF), tetrabromobisphenol A (TBBPA) with Bisphenol A (BPA)**

Bisphenol A was found to be a testicular toxicant in animal models. Bisphenol S (BPS), bisphenol AF (BPAF), and tetrabromobisphenol A (TBBPA) were recently introduced to the market as alternatives to BPA. However, toxicological data of these compounds in the male reproductive system are limited so far. We applied validated an automated multi-parametric high-content analysis (HCA) to characterize and compare the testicular toxicities of BPA and three selected commercial available BPA analogues,

BPS, BPAF and TBBPA. HCA revealed BPAF and TBBPA exhibited higher spermatogonial toxicities as compare with BPA and BPS, including dose- and time-dependent alterations in nuclear morphology, cell cycle, DNA damage responses, and perturbation of the cytoskeleton. Most significantly, among all chemicals tested, BPAF showed significant induction of γH2AX at multiple time-points, suggesting a greater genotoxicity, as compared to other bisphenols. This multi-dimensional toxicological profiling revealed differential testicular toxicities of BPA and its analogues, whereas BPAF and TBBPA showed greater cytotoxicity, followed by BPA and BPS. These results suggested the potential risk of worker exposure to these new alternative compounds. Further safety and risk assessment should be followed.

## Translation of Findings.

Occupational exposure to reproductive toxicants occurs via inhalation, skin absorption, or ingestion. Limited or no toxicological information including reproductive and developmental (R/D) toxicity is available for many industrial chemicals. This application established a "mini-testis" model from testicular cell lines, eliminated a need for animal testing. This research project has established several pathway-based in vitro assays that will be a cost-efficient screening tool for potential R/D toxicity of chemicals and establish exposure limits for effective prevention of R/D toxicity in workplaces such as Manufacturing, Mining, Oil and Gas Extraction and Public Safety.

## Outcomes/ Impact.

1. **potential outcomes, i.e., findings, results, or recommendations that could impact workplace** risk if used;

As discussed previously, the output of the project proposed is the establishment of a pathway-based *in vitro* mini-testis model, this model provides cost-efficient screen tool for potential R/D toxicity of chemicals in the workplace, and provide importance data for establishing exposure limit in workplace for effective prevention of R/D toxicity in workplace.

The research proposed has generated 12 publications, 9 conference proceedings, and generated testicular toxicity data regarding the chemicals in workplace, and provided data for risk assessment. This funding opportunity also supported the career development of Dr. Yu in reproductive toxicology, his long-term effort in seeking and promoting *in vitro* animal alternatives. Therefore, this proposal meets the mission of Cancer, Reproductive, and Cardiovascular Research Program (CRC).

2. **intermediate outcomes, i.e., how findings, results, or recommendations have been used by others to influence practices, legislation, product design, safety management program and training and so forth; and**

Our proposed research is critical to allow in vitro model to become part of an integrated testing battery for R/D toxicity assessment. It's of great importance to build such a test battery for R/D toxicity to fulfill the goal set by the National Research Council (NRC) in the report of "Toxicity Testing in the 21st Century" and to successfully implement these new methodologies in the toxicity testing and predictions [1]. We believed we have established a novel mini-testis model using the testicular cell lines could lead to be an "Approved" animal alternative approach in R/D toxicity assay.

3. **End outcomes, i.e., how findings, results, or recommendations have contributed to documented reductions in work-related morbidity, mortality, and/or exposure.**

The establishment of a pathway-based *in vitro* mini-testis model provides cost-efficient screen tool for potential R/D toxicity of chemicals in the workplace. It will provide importance data for establishing exposure limit in workplace for effective prevention of R/D toxicity in workplace such as MANUFACTURING, MINING, OIL AND GAS EXTRACTION and PUBLIC SAFETY. The ultimate goal of the research by providing a cost-efficient screen tool to identify R/D toxicants in the workplace will significantly improve the risk assessment of reproductive toxicity in the workplace. The identification of reproductive toxicants will reduce the risk of reproductive malfunction of hazardous exposures.

*Section 2 of the Final Progress Report*

## Scientific Report

### Background for the project

Occupational exposure to reproductive and developmental (R/D) toxicants may occur via inhalation, skin absorption, or ingestion. Thousands of chemicals exist in the workplace and there is limited or no toxicological information available. Furthermore, even for compounds for which there is toxicological testing data, the data often do not include assessment of the effects on R/D effects since toxicity testing on animals is so expensive. In addition, extrapolating the adverse effects of animal toxicity studies to humans is significantly confounded by dose-response effects and by cross-species differences in sensitivity and susceptibility. Currently, only a few agents have been identified as being definitely capable of producing structural abnormalities in humans in the absence of maternal toxicity [2]. Only a few agents such as dibromochlorpropane and 2-bromopropane have been discovered to affect human spermatogenesis just due to the occupational hazard accidents in workers [3]. Subsequent animal experiments confirm their reproductive toxicity in animals [4-23]. Risk assessment for R/D toxicity is particularly challenging since the system is highly complex, and *in vivo* tests such as two generation studies use a large number of animals [24, 25].There are thousands of chemicals in the workplace, and only a few of them could be recommended for testing under the NIEHS Health Assessment and Translation Program (Formerly CERHR). Since the report “Toxicity Testing in the 21st Century” by the National Research Council (NRC, 2007) envisioned that *in vivo* animal testing can eventually be replaced by a combination of *in silico* and *in vitro* approaches [1], the demand to identify *in vitro* models for R/D toxicity testing has grown [26, 27]. Over the years, some alternative methods have been developed as a part of the test battery in assessing R/D toxicity, but the majority are focused on embryotoxicity testing such as the embryonic stem cell test (EST), the whole embryo culture test (WEC), and the limb bud micromass (MM) [28-31], but not on *in vitro* assays targeting processes such as spermatogenesis. After years of animal studies with 2-bromoprane and 1-bromoproane, we realized the importance of creating alternative testing for cost-efficient screen of R/D toxicity, and developed a three-dimensional testicular cells co-culture system (3D-TCCS) from rat and have applied this model to examine the mechanisms of toxicity of testicular toxicants cadmium and phthalates [32, 33]. Our studies demonstrated that this 3D-TCCS can discriminate known developmentally toxic phthalate esters (PEs) from non-toxic PEs [34-37]. However, this novel approach still employs a large number of animals for the isolation of testicular cells. In this project, we examined and established a 3D-TCCS from established testicular cell lines. We optimized protocol for the establishment of mini-testis. Finally, we tested the 3D-TCCS with a list of “gold standard testing compounds” and tested blindly the predictability of these assays. We also developed pathways-based assays, directly linked to the endpoint of male reproductive toxicity, including abnormal spermatogenesis and male infertility. Three specific aims have been tested in this project periods as originally planned, and no changes were made.

**Specific Aim 1: To examine and optimize *in vitro* 3D-TCCS model from testicular cell lines.**

*In vitro* culture systems have been used to evaluate testicular changes during normal development [38-43]. I*n vitro* culture systems for successful differentiation of germ cells require Sertoli cells [44]. Sertoli/ gonocytes co-cultures (SGC) are used to examine the interactions and effects of hormones and growth factors on spermatogonia survival and proliferation *in vitro* [45, 46]. Spermatogonia stem cells such as immortalized spermatogonia have proven to be useful in screening reproductive toxicants [47, 48]. However, they are of limited use in toxicological studies [49, 50]. It has been shown that spermatogonia cell self-renewal and progeny production is probably controlled by the neighboring differentiated cells and extracellular matrix (ECM), known *in vivo* as niches. Coating tissue culture-treated dishes (2-D substratum) with ECM Matrigel*TM* to enhance Sertoli cell attachment been used with relative success in culture of SGC [39, 50, 51]. We have built upon these studies and have developed an *in vitro* co-culture model (3D-TCCS) from rat [32, 33]. This 3D-TCCS provides a significant improvement over existing 2D substratum approach used in co-culture [32, 33]. This 3D-TCCS is a scale down of *in vivo* testis and includes three major testicular cells (germ cells, Sertoli cells, and Leydig cells). ECM overlay permits formation of a testicular-like multilayered architecture that mimics *in vivo* characteristics of seminiferous tubules [32, 33]. The 3D-TCCS from rat is proved to be a valuable *in vitro* model to screen R/D toxicity [35-37]. However, this 3D-TCCS still has its disadvantage in employing animals for the isolation of testicular cells, far away to the establishment of animal-free testing system. *In vitro* culture systems have been used to evaluate testicular changes during normal development [38-44]. Sertoli/gonocytes co-cultures (SGC) are used to examine cell-cell interactions, and effects of hormones and growth factors on spermatogonia survival and proliferation *in vitro* [45, 46]. Self-renewal and progeny production of spermatogonia is controlled by the neighboring differentiated cells and extracellular matrix, known as substrate *in vivo* niches and Sertoli cells are required to the successful differentiation of germ cells *in vitro* culture systems [44]. ECM Matrigel-based primary testicular cells model was reported to form a testicular-like multilayered architecture that mimics *in vivo* characteristics of the seminiferous tubules [32, 33, 52-55]. As previously demonstrated, this model differentially responds to various phthalates exposure with the changes of several cellular pathways, showing sensitive response to testicular toxicity [35, 52, 55]. However, this *in vitro* primary testicular cells co-culture still has its disadvantage in employing animals for the isolation of these testicular cells and the complicated isolation procedure leads to inconsistency of these primary testicular cells [54]. Therefore, as proposed, we examined and optimized the protocol for the establishment of the in vitro mini-testis for the R/D toxicity testing. We created a *niche* environment in which spermatogonial stem cells can be maintained and directed to proliferate and undergo meiosis and complete spermatogenesis. We developed and constructed an *in vitro* testicular cell co-culture model from rodent testicular cell lines including spermatogonial stem cells (SSC), Sertoli cells, and Leydig cells.

**Cell cultures and Treatments*:*** mouse Leydig cells (TM3) and Sertoli cells (TM4) were purchased from ATCC. The mouse C18-4 spermatogonial cell line (SPA) was established from germ cells isolated from the testes of 6-day-old Balb/c mice. This cell line shows morphological features of type A spermatogonia, expresses germ cell–specific genes such as GFRA1, Dazl and Ret, which are markers specific for germ cells in the testis [56, 57]. Leydig cells and Sertoli cells were cultured in DME/F12 medium supplemented with 1% streptomycin and penicillin, 5% horse serum, and 2.5% FBS, and maintained at 33˚C with 5% $CO_2$. SPA cells were cultured in DMEM/high glucose medium supplemented with 5% FBS and were maintained at 33˚C with 5% $CO_2$ [56]. For a single cell culture model, cells were seeded to 96-well plates at the density of 2.0 x$10^4$ per well. For testicular cell co-culture model, we mimicked the cellular composition of mouse testis around Day 5 of newborn mice, and the percentage of each cell type during this period are approximately 80%, 15% and 5% for gonocyte, Sertoli cell, and Leydig cells, respectively. Gonocyte, Sertoli cell, and Leydig cells were mixed based on above proportion and seeded into 96-well plate in DMEM/high glucose medium at 33˚C, supplemented with 5% nu-serum. ECM Matrigel (Corning, New York) was added to each dish for a final concentration of 100 µg/ml and the plates were gently swirled to ensure dispersal of

Matrigel after addition. Cells were cultured overnight and treated with various concentrations of testing compounds for the indicated doses and time periods.

**Assessment of cell morphology:**

All cultures were viewed with a Olympus inverted microscope equipped with phase-contrast optics (Olympus, Tokyo, Japan) at intervals during culture to assess their general appearance. Resultant images were captured and digitized with a Nikon Camera. To further examine the morphology of the cultured cells, a multi-parametric fluorescence assay was applied to visualize the cytoskeleton, nuclear shape and cell proliferation. Cells were washed with phosphate buffered saline (PBS) 72 h and fixed with 4% formaldehyde for 20 min, and then washed three times with PBS. After permeabilization in TBS containing 0.5% Triton X-100 (TX-100) for 10 min, cells were blocked for 30 min in 5% normal goat serum (NGS; Sigma) in PBS with 0.1% TX-100, and then incubated with primary Phospho-Histone H3 (Ser10) Antibody **(**1:200, Fisher Sci) in PBS with 1% goat serum and 0.1% TX-100 over night at 4°C. Cells were washed three times in PBS before the addition of a goat anti-rabbit Alexa-conjugated secondary antibody (1:200 dilution, Molecular Probes, Inc. Eugene, OR) for 1 h at 37°C. FITC-conjugated phalloidin (1 µg/ml, Sigma) and 2 µl Hoechst 33342 (1 mg/ml) was added to each dish to stain the F-actin and the nuclei. The stained co-cultures were captured in Arrayscan VTI. The method is based on a three-channel assay, which uses a 20× objective (NA 0.5), a Hamamatsu ORCA-ER digital camera in combination with a 0.63× coupler and Carl Zeiss microscope optics for automatic image acquisition. Images were acquired in high resolution (1024 × 1024) and auto focus mode. Channel one applies the BGRFR 386-23 for Hoechst 33342, which was the focus channel, and the objects (nuclei) were identified.

**Results and Outcomes:**

We established a testicular cells co-culture model using testicular cell lines including spermatogonia, Sertoli cell and Leydig cells (Fig.1), which is based on the cellular composition of mouse testis around Day 5 of newborn mice. Cells in a defined proportion were seeded in a 96-well plate for high-throughput analysis. A non-serum culture medium including DMEM (Hyclone) supplemented with 10% Nu-serum was used. Furthermore, ECM overlay significantly improved the culture to form a 3D structure (Fig 1A). Fig. 1 illustrates the 3D co-culture structure72 h (A) after seeding. Multi-parametric staining of the cells was conducted to demonstrate the morphology, with nuclear stained blue, and cytoskeleton stained green with f-actin and phosphor-histone 3 staining red. As shown in Fig1B, single culture of Spermatogonia did not form a 3D-like testicular structure. In summary, we established the 3D TCSS from testicular cell lines, and optimized co-culture condition through the morphology and cellular markers.

**Discussion**

Spermatogenesis is a dynamic and well-characterized process, which occurs within an ordered and structural biological context for molecular, genetic, epigenetic, functional, and morphological events. The establishment of an ideal culture system in which spermatogonial

stem cells can proliferate and undergo meiosis and complete spermatogenesis is under

**Figure 1** Comparison of morphology of testicular cell co-culture mode (A) l versus single spermatogonia culture (B). Testicular cell co-culture model consisted of three cell types: Spermatogonia A cells, Leydig cells and Sertoli cells. Cells were fixed 72 h after culture, and fixed and stained with f-actin and phosphso-histone h3. Automated multi-channel images were acquired using ArrayScan VTI with X 40 magnification (Thermo-Fisher Sci).Multi-channel analysis shows nuclear (Hoechst 33342, blue), cytoskeleton f-actin (phalloidin, green), and phosphso-histone h3 (pink), as early mitotic marker. Three dimensional structure was formed in the co-culture model, but not in the single spermatogonia cell culture.

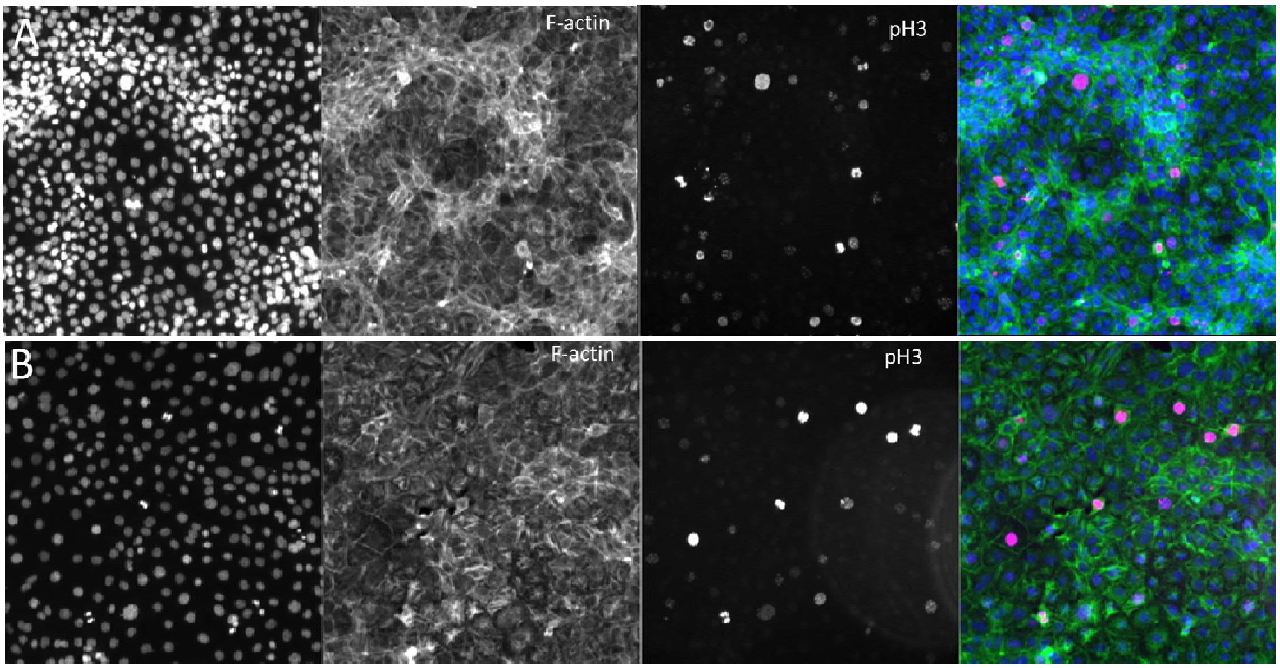


**Figure 2.** In vitro "mini-testis" model from testicular cell lines including Spermatogonial stem cell, TM4 Sertoli cells and TM3 Leydig cells with ECM. Multi-parametic analysis shows nuclear (Hoechst 33342, blue), cytoskeleton f-actin (phalloidin, green), and phospho-γH2AX (pink), as early DNA damage marker. Cadmium treatment for 48 h shows disruption of the actin cytoskeleton, and induce phosphorylation of γH2AX, a sensitive molecular marker of DNA damage.

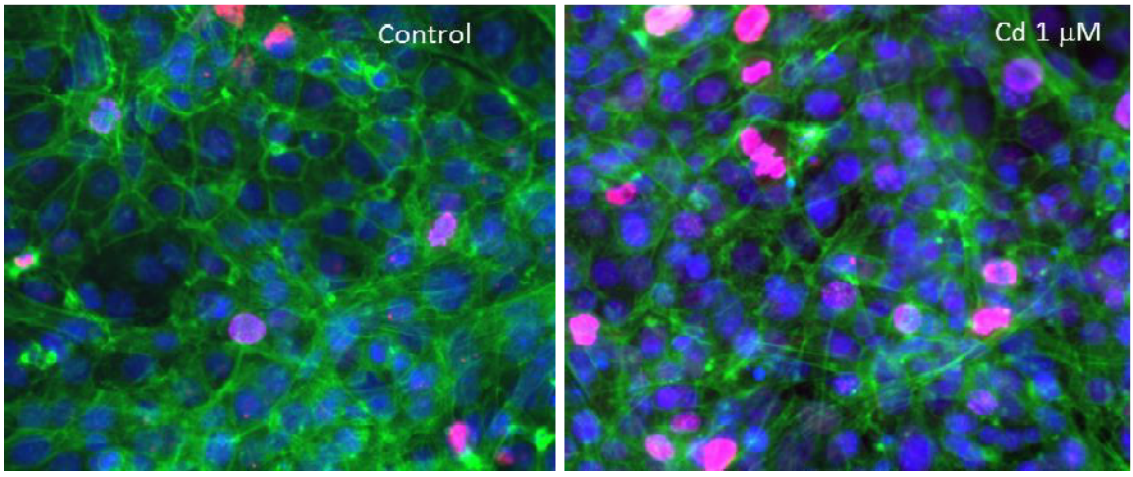


intensive study [67]. Attempts to achieve the differentiation events characterizing mammalian spermatogenesis during *in vitro* culture of immature germ cells have been reported since the early 1960s [68-70]. These studies demonstrate that *in vitro* co-culture conditions are the key to

successfully model the proliferation of spermatogonia and differentiation of meiotic prophase spermatocytes into secondary spermatocytes. Within the co-culture system, an organotypic environment that mimics *in vivo* conditions provides critical cell-cell interactions between germ cell, Sertoli, and Leydig cells.

**Specific Aim 2: To establish a toxicity-based high throughput 3D-TCCS model for R/D toxicity evaluation.**

We tested this animal-free *in vitro* testicular co-culture model with 32 selected compounds and compared to any single cell culture of spermatogonia, Sertoli cell or Leydig cells. The comparison between the *in vitro* toxicity (IC50 of cell viability) and *in vivo* reproductive toxicity (lowest observed adverse effect level on the reproductive system) was conducted. We observed a strongest correlation of IC50 of the cell viability between this *in vitro* testicular co-culture model and *in vivo* testing results, but not with any single testicular cell culture models. We have demonstrated that our *in vitro* co-culture model may be useful in screening testicular toxicants in a wide concentration range and prioritize chemicals for future experiments.

**Test compounds for validation:**

A variety of chemicals have been listed as potential agents that might impair reproduction and development. We will choose well-recognized R/D toxicants, each of which has been critically reviewed by the NIEHS/NTP expert panel. A set of “gold standard” reference compounds is essential for use as benchmarks for validation of new assays [58]. These compounds should have known *in vivo* toxicity profiles including structural and mechanistic information and represent several forms of toxicity and also be freely available. Currently there is no such single list of compounds available for R/D toxicity testing validation. However ECVAM has sponsored an international validation study to assess the R/D tests [58] and these compounds will also be used for validation. A database of i*n vivo* and *in vitro* developmental toxicity test results was compiled on 310 chemicals, and a final list of 20 compounds including strongly embryotoxic (A class), weakly embryotoxic (B class), and non-embryotoxic (C class) were recommended [58]. Based on the *in vivo* animal studies conducted by NIEHS/NTP, a group of experts reviewed the R/D toxicity of chemicals, and set priorities for further risk assessment [59]. A total of 45 compounds were identified as R/D toxicants [59-61]. Based on these lists, we selected 32 compounds and tested in our *in vitro* model (Table 1).

**Neutral red (NR) dye uptake assay**

Cell viability was determined by measuring the capacity of cells to take up NR [62-64]. NR can be retained inside the lysosomes of viable cells, while the dye cannot be retained if the cells dies. Dye retention is proportional to the number of viable cells, and can be measured based on NR absorbance [63, 64]. Cells were seeded to 96-well plates. Cells were treated with different compounds at 4 concentrations with 5 replicates for each concentration. After 24 h or 48 h, the medium was replaced with a medium containing NR dye (50μg/cm$^3$, 200μl per well). After incubation for 3 h, supernatants were removed and the cultures washed with PBS twice. The cells were then fixed with 200 μl 1% acetic acid-50% ethanol-50% distilled water. The plates were shaken for 10 min at room temperature and the absorption was measured at 540nm with a Synergy HT microplate reader (BioTek, VT). Cells treated with vehicle (0.05% DMSO) were used as the reference group with cell viability set as 100%. Cell viability was expressed as percentage of the mean of vehicle controls after subtracting the background control. Initial testing concentration of these compounds were determined based on published cytotoxicity data. After examination of the initial dose-response curve from our co-culture model, the dose-range was adjusted. For those compound with low cytotoxicity, the highest

concentrations tested were 50 mM and 5 mM for water-soluble or lipophilic chemicals, respectively.

**Table 1. Listed chemicals for in *in vitro* testing**

| Chemical Name | Abbreviation | CAS NO. | Molecular Weight | Purity (%) | Application | Supplier |
|---|---|---|---|---|---|---|
| Sodium arsenite | Ar | 7784-46-5 | 129.91 | 90 | Pesticides | GFS |
| Boric acid | BA | 10043-35-3 | 61.83 | 99.5 | Insecticide | Sigma |
| Benzyl butyl phthalate | BBP | 85-68-7 | 312.36 | 98 | Plasticizer | Sigma |
| Benzophenone-3,3′,4,4′-tetracarboxylic dianhydride | BEN | 2421-28-5 | 322.23 | 96 | Solvent | Sigma |
| 2,2-Bis(4-hydroxy-3-methylphenyl)propane | BPA | 80-05-7 | 256.34 | 99 | Plasticizer | Sigma |
| 4,4'-(Hexafluoroisopropylidene)diphenol | BPAF | 1478-61-1 | 336.23 | 97 | Fire-retd plasticizer | Sigma |
| 4,4′-Sulfonyldiphenol | BPS | 80-09-1 | 250.27 | 98 | Flame retardant | Sigma |
| Cadmium chloride | Cd | 10108-64-2 | 183.32 | 99.99 | Dye | Sigma |
| Chlorpyrifos | CHL | 2921-88-2 | 350.59 | NA | Pesticides | ce |
| Cyclophosphamide | CYC | NA | 279.1 | NA | Cancer | TCI |
| Dibutyl phthalate | DBP | 84-74-2 | 278.34 | 99 | Solvent | Sigma |
| Dioctyl phthalate | DEHP | 117-81-7 | 390.56 | 99.5 | Plasticizer | Sigma |
| Diethylphthalate | DEP | 84-66-2 | 222.24 | 9935 | Plasticizer | Sigma |
| Diethylstilbestrol | DES | 56-53-1 | 268.35 | 99 | estrogen | Fisher |
| Diazinon | DIA | 333-41-5 | 304.35 | NA | Pesticides | Chemservi |
| Dimethyl phthalate | DMP | 131-11-3 | 194.18 | 99 | Plasticizer | Sigma |
| Dioctyl terephthalate | DOTP | 6422-86-2 | 390.56 | 96 | Plasticizer | Sigma |
| Dipentyl phthalate | DPP | 131-18-0 | 306.4 | 99 | Plasticizer | Sigma |
| β-Estradiol | ES | 50-28-2 | 272.38 | NA | Estrogen therapy | Sigma |
| Hexachlorophene | HEP | 70-30-4 | 406.9 | NA | Skin cleanser | Fisher |
| Heptachlor | HEX | 76-44-8 | 373.32 | NA | Pesticides | Fisher |
| Hydroxyurea | HU | 127-07-1 | 76.05 | 98 | Sickle cells | Sigma |
| 2-methoxyethanol | ME | 109-86-4 | 76.09 | 99.8 | Solvent | Sigma |
| Parathion | PARA | 56-38-2 | 291.26 | NA | Pesticides | ce |
| Saccharin Sodium | SAC | 128-44-9 | 205.17 | NA | Sweetener | Sigma |
| 3,3',5,5'-Tetrabromobisphenol A | TBBPA | 79-94-7 | 543.87 | 97 | Flame retardant. | Sigma |
| Tri-(2-chloroethyl)phosphate | TCEP | 115-96-8 | 285.49 | 97 | plasticizer | Sigma |
| Tricresyl phosphate | TCP | 1330-78-5 | 368.36 | 90 | Plasticizer | Sigma |
| 2,4,4′-Trichloro-2′-methoxydiphenyl ether | TCS | 3380-34-5 | 303.57 | NA | Bateria resistance | Sigma |
| Vinclozolin | VIN | 50471-44-8 | 286.11 | NA | Pesticides | Fisher |
| Valproic acid sodium salt | VPA | 1069-66-5 | 166.19 | 98 | Anticonvulsant | Sigma |
| Zearalenone | ZEA | 17924-92-4 | 318.36 | NA | Pesticides | Sigma |

### *In vivo* reproductive toxicity data and comparison

Based on the review of U.S Environmental Protective Agency's office of Pesticide program, reproductive lowest observed adverse effect levels (rLOAEL) of rats were established to indicate chemicals' reproductive toxicities (http://actor.epa.gov/actor/faces/ACToRHome.jsp). The endpoints for determining rLOAEL of rats includes but not limited to primary fertility, early offspring survival, offspring weight, longer-term offspring survival and other systemic offspring toxicities. As previously reported, i*n vivo* reproductive toxicants *in vivo* were defined as having achieved an rLOAEL lower than 500 mg/kg/day while *in vitro* reproductive toxicants were defined here as having achieved a half maximal inhibitory concentration ($IC_{50}$) ≤ 1,000 μM [65].

Compounds with insufficient *in vivo* reproductive toxicity data were marked “NA” for “no available information”. Chemicals with a positive or negative test result in a NR assay and positive or negative literature evaluation were used in the calculations of concordance (percentage of results from the NR assay that match the calls from the literature [66]. In addition, sensitivity (%) was calculated from the formula: 100 × (the proportion of chemicals with a positive result in an NR assay that were positive based on the literature calls). Similarly, specificity (%) was derived from the formula: 100 × (the proportion of chemicals with a negative result in a NR assay that were negative based on the literature). The “NCs” were not included in these calculations of sensitivity, selectivity, or concordance.

**Statistical analysis**:

The cell viabilities were calculated as the arithmetic mean percentages of treated versus the control. The data represented the average ± standard deviation of five replicates, and were expressed as a percentage of the treated versus untreated control. $IC_{20}$, $IC_{50}$, $IC_{84}$, and $IC_{90}$ values were calculated using survival analysis and the PROBIT method with StatPlus software (AnalystSoft Inc., Walnut, CA). The individual $IC_{50}$ values were assessed among the cell types by a one-way analysis of variance (ANOVA) at significance level 95%, $\alpha = 0.05$ to determine the differences among the cells ($p < 0.05$). Correlation between $IC_{50}$ values between the cell types was also performed to establish in vitro–in vivo correlation. The relationship between $IC_{50}$ values and rat rLOAEL values was evaluated using linear regression. The Pearson correlation coefficient between $IC_{50}$ values and rLOAEL was calculated using GraphPad 5.0 (La Jolla, CA). Hierarchical clustering analyses were conducted based on the average linkage and elucidation distance correlation coefficients using MeV software. Correlation of $IC_{50}$ values against published *in vivo* toxicity data was established to determine the predictability of the in vitro results compared to in vivo toxicity. The degree of correlation was examined based on the *r* value and regression coefficient ($R^2$).

**Results and Outcomes:**

**Cell viability changes of co-culture induced by 32 chemicals.**

In order to examine whether this *in vitro* co-culture model can be used to screen testicular toxicants, we first compared the cytotoxicity with known and unknown reproductive toxicants (Table 1). We applied Neutral red up-taken assay to examine the dose-dependent curves for 24 h and 48 h treatment with those selected compounds in the co-culture model as well as a single cell culture model including spermatogonia C18 cell, Sertoli cell and Leydig cell. Figure 2 shows the dose-dependent cytotoxicity in response to 32 compound in the co-culture model after 48 h treatment (Figure 2). These compounds were organized into four charts based on their highest concentrated tested. Figure 2A included compounds whose highest tested concentrations ≤ 100 μM, including ZEA, Cd, As, HEP, DES, BPAF, TBBPA, and HEX. ZEA, As and Cd were most toxic followed by HEP, DES, BPAF, TBBPA and HEX. Figure 2B shows the dose-dependent cytotoxicity of phthalate esters. Male developmentally toxic phthalate esters including DBP, DEHP, BBP and DPP induced a dose-dependent decrease of cell viability after treatment for 48 h while non-toxic phthalate esters including DEP, DMP and DOTP induced no or slight decrease of cell viability. Figure 2C show a group of compounds including TCS, CHL, DIA, BPA, BPA, PARA, BEN and ES, with the highest concentration tested ranged from 100μM to 500μM. TCS, CHL, DIA and BPA induced significantly dose-dependent decrease of cell viability (Fig. 2C) while no significant decreases of cell viability were observed for BEN an BEN. Fig. 2D listed those tested compounds with a low-cytotoxicity with the highest concentrations tested ranged from 5 mM to 50 mM. HU, TCP, VIN, TCEP, BA and VPA statistically significantly decreased the cell viability while other compounds including

CYC, VPA, ME and SAC did not cause significant decrease in cell viability across all concentrations.

**Figure. 2. Cell viability after tested with selected compounds in the co-culture model for 48 h.** The co-cultures were seeded in a 96-well plate for 24 h before treatment with chemicals at different concentrations for 48 h. Cell viability assessments were conducted using NR dye uptake assay. Data are presented as mean ± SD of five replicates.

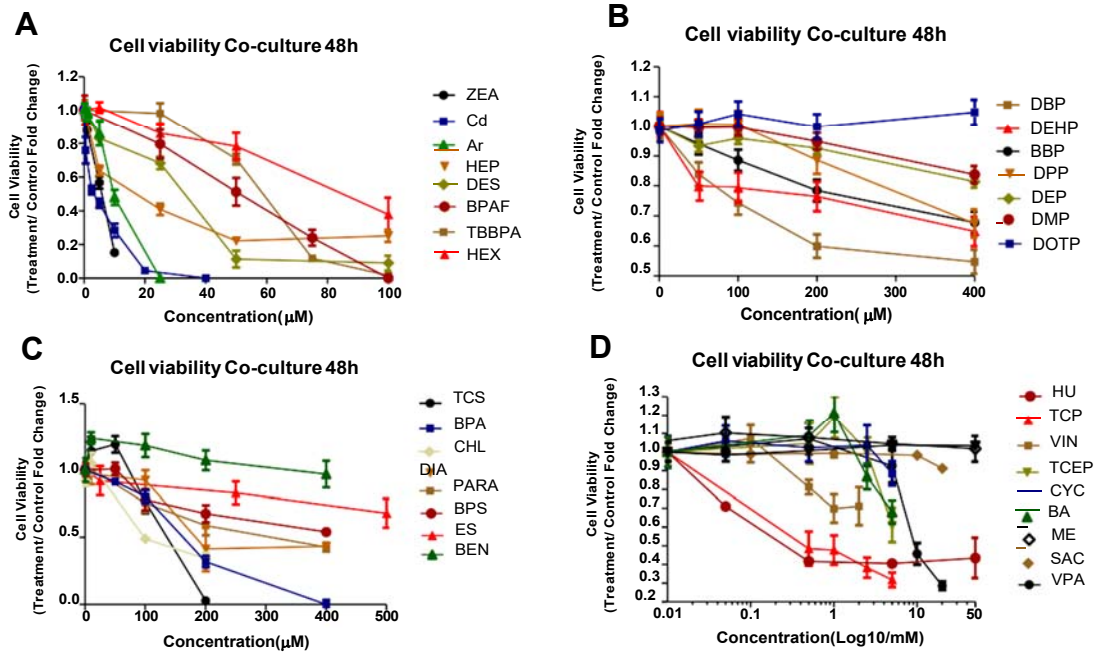


### $IC_{50}$ of chemicals.

The $IC_{50}$ values of tested compounds in the co-culture model, and single cell culture models treated for 24 and 48 h were listed in Table 2. As indicated in the Table 2, the $IC_{50}$ values for the 24 h treatment were generally higher than those for the 48 h treatment. The $IC_{50}$ values for Cd, ZEA, As, HEP, DES, TBBPA, TCS, HEX, and CHL were mostly ≤ 100 μM. The $IC_{50}$ values of chemicals in the second and third group (Fig.3B-C) were mostly ≤ 1,000 μM. For chemicals in the fourth group (Fig. 3D), the toxicities were too low to derive IC50 values from the simulation, therefore, the highest concentration tested were used. When comparing different cell types, different sensitivities to the same chemical were observed. In general, the lower the $IC_{50}$ value, the more sensitive the cell type is. Our results showed that Sertoli cells were more sensitive to BPS, PARA, and TCP. Spermatogonia A cells were sensitive to Cd, As, and HEX. Both Sertoli cells and Leydig cells were sensitive to BPA, BPAF, and HEP.

### Cluster analysis

In order to compare the testicular toxicity among all tested chemicals within our model, a non-supervised two-dimensional hierarchical cluster analysis of the $IC_{20}$, $IC_{50}$, $IC_{84}$, and $IC_{90}$ values of the co-culture after a 48 h treatment was employed (Fig. 3). The figure illustrates the degree to which the chemicals affected cell viability. The chemicals at the top (cluster 1) were the most toxic, and those at the bottom (cluster 3) were the least toxic. Cluster1 included Cd, ZEA, As, HEP, DES, TBBPA, TCS, HEX, and CHL, all of which belong to the first group (Fig.

2A). Cluster 2 included BPAF, HU, BPA, DIA, DPP, BPS, DBP, BBP, BEN, PARA, DEHP, VPA, and ES, mainly chemicals in the second and third groups (Fig. 2B and Fig. 2C). Cluster 3 included non-toxic phthalate esters DOTP, DEP, DMP and VIN, ME, CYC, TCEP, BA, and SAC.

### Correlation between $IC_{50}$ and in vivo reproductive toxicity

**Table 2. $IC_{50}$ values of tested chemicals in co-culture and single cell types at 24h and 48h.**

**Cell viabilities from NR dye uptake assay were calculated by dividing mean optical density (OD) values o treatment group by control group after subtracting the blanks (no cells). IC50 were derived from dose-response curves with StatPlus using survival analysis and the probit method. For chemicals that the cell viability did not achieve 50% decrease at the highest treatment concentration, the highest concentratio was assigned as $IC_{50}$.**

| | IC50 (μM) | | | | | | | |
|---|---|---|---|---|---|---|---|---|
| Chemical | Co-culture | | Spermatogonia A | | Leydig cells | | Sertoli cells | |
| | 24h | 48h | 24h | 48h | 24h | 48h | 24h | 48h |
| ZEA | 7.2 | 7.1 | 9.3 | 3.6 | 3.4 | 2.5 | 3.1 | 2.5 |
| OH | 11.3 | 4.2 | 2.1 | 2.1 | 18.0 | 6.5 | 14.8 | 0.5 |
| Ac | 15.0 | 10.0 | 8.0 | 8.6 | 20.3 | 16.1 | 12.0 | 8.0 |
| HEP | 10.7 | 11.4 | 100.0 | 20.0 | 2.6 | 0.8 | 3.0 | 2.7 |
| DES | 31.1 | 20.0 | 25.5 | 16.0 | 32.4 | 25.0 | 26.0 | 24.1 |
| TBBPA | 70.0 | 38.0 | 74.0 | 35.0 | 70.0 | 30.0 | 30.0 | 36.0 |
| TCS | 121.0 | 78.5 | 82.7 | 57.3 | 135.0 | 60.0 | 61.0 | 72.7 |
| BPAF | 76.0 | 30.0 | 70.0 | 35.5 | 30.0 | 20.0 | 32.4 | 22.3 |
| HEX | 63.1 | 62.0 | 22.0 | 5.0 | 60.0 | 30.0 | 35.0 | 44.0 |
| OHL | 91.5 | 60.0 | 116.0 | 08.0 | 142.0 | 120.0 | 212.0 | 120.0 |
| HU | 1000.0 | 200.0 | 1000.0 | 200.0 | 600.0 | 200.0 | 300.0 | 180.0 |
| BPA | 210.0 | 168.0 | 100.0 | 164.5 | 66.0 | 60.5 | 60.0 | 70.0 |
| DIA | 270.0 | 222.0 | 303.0 | 200.0 | 268.0 | 250.0 | 269.0 | 227.0 |
| BPS | 574.0 | 341.0 | 805.0 | 357.0 | 436.0 | 400.0 | 211.0 | 74.3 |
| DPP | 350.0 | 352.5 | 400.0 | 372.0 | 400.0 | 244.0 | 400.0 | 400.0 |
| DBP | 437.0 | 387.5 | 400.0 | 371.0 | 400.0 | 400.0 | 400.0 | 400.0 |
| PARA | 490.0 | 400.0 | 343.0 | 207.2 | 400.0 | 400.0 | 264.0 | 117.5 |
| TCP | 3000.0 | 400.0 | 2020.0 | 1697.0 | 3000.0 | 800.0 | 208.0 | 183.0 |
| BBP | 695.0 | 536.0 | 400.0 | 400.0 | 400.0 | 400.0 | 400.0 | 400.0 |
| DEHP | 881.0 | 400.0 | 827.0 | 400.0 | 400.0 | 400.0 | 400.0 | 400.0 |
| DCN | 400.0 | 400.0 | 400.0 | 400.0 | 400.0 | 400.0 | 400.0 | 400.0 |
| ES | 1000.0 | 1000.0 | 1000.0 | 280.0 | 1000.0 | 027.0 | 1000.0 | 1000.0 |
| VIN | 4000.0 | 3800.0 | 1766.0 | 880.0 | 2000.0 | 2000.0 | 2000.0 | 2000.0 |
| BA | 8378.0 | 8071.0 | 8000.0 | 3602.3 | 16954.0 | 15823.0 | 8000.0 | 8000.0 |
| TCEP | 8000.0 | 8000.0 | 8111.0 | 3876.0 | 8000.0 | 8000.0 | 8000.0 | 8000.0 |

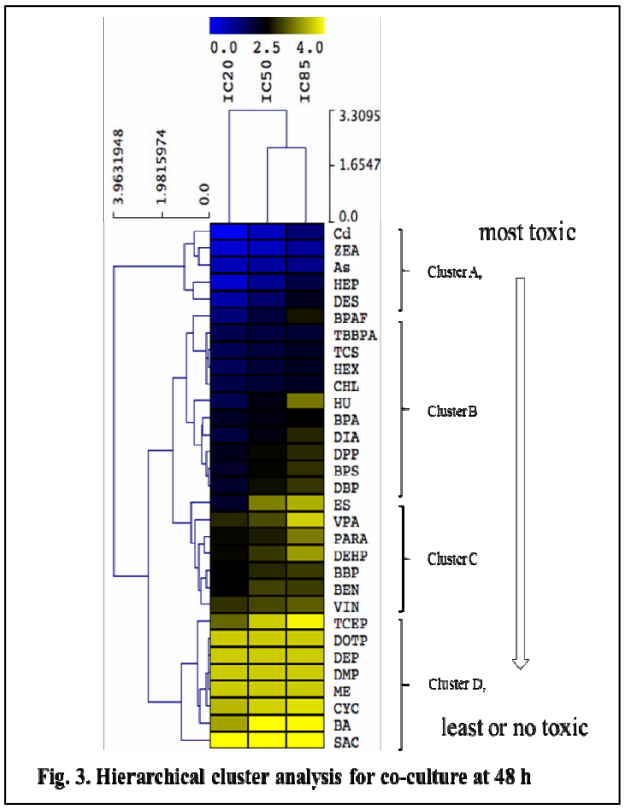


Fig. 3. Hierarchical cluster analysis for co-culture at 48 h

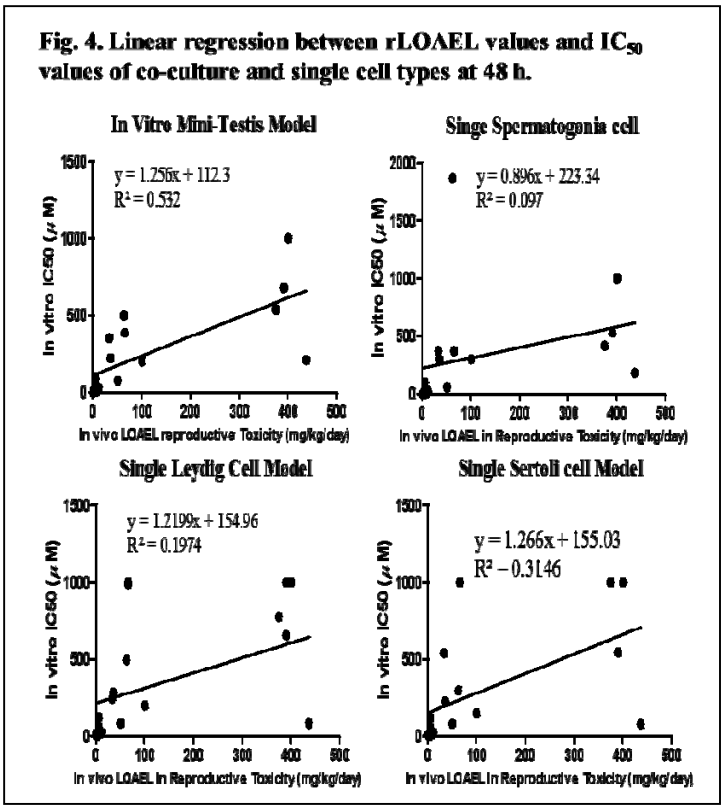


The rLOAEL value indicates the reproductive toxicity *in vivo*. Among the 32 tested compounds, eighteen of them had a reported *in vivo* rLOAEL value, and correlation between *in vitro* IC50 was examined to determine what extent an *in vitro* $IC_{50}$ could predict an *in vivo* rLOAEL[65]. $R^2$ values for the co-culture model, Spermatogonia cells, Leydig cells and Sertoli cells for the 24 h treatment were 0.43, 0.03, 0.04, and 0.2, respectively. For 48 h exposures as shown in Figure 4, the, the $R^2$ values for the co-culture model, spermatogonia cells, Leydig and Sertoli cells were 0.53, 0.1, 0.19, and 0.31, respectively. The co-culture model had the highest $R^2$ value as compared to any single cell culture model for both 24 h and 48 h treatments.

Pearson's correlation coefficient and the *r*-values for the co-culture model, Spermatogonia cells, Leydig cells, and Sertoli cells for the 24 h treatment were 0.66, 0.16, 0.21, and 0.48, respectively. For 48 h exposures, the *r*-values were 0.73, 0.31, 0.44, and 0.56. The co-culture displayed higher *r*-values than any single cell types for both 24 h and 48 h treatment.

**Concordance, sensitivity and specificity**

The concordance, sensitivity, and specificity were listed in Table 3. rLOAEL values were used to call the *in vivo* reproductive toxicity. DIA, DES, Cd, CHL, HU, HEP, HEX, As, BPA, TBBPA, TCS and ZEA were positive *in vivo* and also positive for all the *in vitro* culture model. ME and VIN were positive *in vivo*, but negative in all in vitro culture models. DEHP, DBP, TCP, BBP, DPP, VPA, TCEP, and PARA displayed different toxicities for different cell types. Table 6 shows that BA, DOTP, DMP, DEP, and SAC were all negative *in vivo* and *in vitro*. There is insufficient data regarding the reproductive toxicity of BPAF, BPS and Ben.

The concordance, sensitivity, and specificity were listed in Table 3 and values were higher at 48 h compared to 24 h for the cell culture models. At 48 h, the co-culture model, when compared to single cell culture mode, displayed the highest concordance, sensitivity, and specificity, at 79.31%, 85.71%, and 62.5%, respectively. The concordance values for

spermatogonia cells, Leydig cells, and Sertoli cells at 48 h were 73.33%, 73.33%, and 67.74%. Similarly, the sensitivity values for spermatogonia A cells, Leydig cells, and Sertoli cells at 48 h were 80.95%, 80.95%, and 76.19%. Specificity values were 55.56%, 55.60%, and 50.00%, respectively. For 24 h, co-culture still had the highest concordance, sensitivity, and specificity values; concordance values for co-culture, Spermatogonia A cells, Leydig cells, and Sertoli cells were 65.63%, 48.57%, 44.44%, and 52.94%. Sensitivity values were 71.43%, 57.14%, 52.38%, and 61.91%. Specificity values were 45.46%, 35.71%, 33.33%, and 38.00%. In summary, the co-culture showed the highest values for concordance, sensitivity, and specificity across all conditions after the 48 h treatment.

Table 3 Comparison of concordance, sensitivity, and specificity of the co-culture model with any single cell culture models.

| | 24 h | | | | 48 h | | | |
|---|---|---|---|---|---|---|---|---|
| | Co-culture | Spermatogonia A | Leydig cells | Sertoli cells | Co-culture | Spermatogonia A | Leydig cells | Sertoli cells |
| Concordance | 65.63% (45.72%, 79.27%) | 48.57% (32.01%, 65.13%) | 44.44% (28.21%, 60.68%) | 52.94% (36.16%, 69.72%) | 79.31% (64.57%, 94.05%) | 73.33% (57.51%, 89.16%) | 73.33% (57.51%, 89.16%) | 67.74% (51.29%, 84.20%) |
| Sensitivity | 71.43% (52.11%, 90.75%) | 57.14% (35.98%, 78.30%) | 52.38% (31.02%, 73.74%) | 69.72% (41.13%, 82.68%) | 85.71% (70.75%, 100%) | 80.95% (64.16%, 97.75%) | 80.95% (64.16%, 97.75%) | 76.19% (57.97%, 94.41%) |
| Specificity | 45.46% (16.03%, 74.88%) | 35.71% (10.61%, 60.81%) | 33.33% (9.48%, 57.19%) | 38% (12.02%, 64.91%) | 62.50% (28.95%, 96.05%) | 55.56% (23.09%, 88.02%) | 55.56% (23.09%, 88.02%0 | 50% (19.01%, 80.99%) |

## Discussion

Continuing our efforts to construct co-culture systems to screen for testicular toxicants, this co-culture system was treated with 32 chemicals in total. Different cell types were then treated with these chemicals. The co-culture and single cell cultures were compared to distinguish a better condition to screen testicular toxic chemicals. Each single cell type is sensitive to a certain category of chemicals; such as Leydig cells, which express androgen receptors, are very sensitive to endocrine disruptors. Due to the complexity of testes, the concentrations that chemicals were toxic to single cell types, were not corresponding to the concentrations *in vivo*. It is proposed that single cell types should not be as representative as co-culture cells that can interactively coordinate different cell types and enables a similar physiological condition in testes. The co-culture, enabling the communication between different cell types, should be a better system than single cell types to screen testicular toxic chemicals. Our hypothesis was confirmed by comparing *in vitro* $IC_{50}$ with *in vivo* rLOAEL of rats. The co-culture offered better correlation with rLOAEL than single cell types through linear regression and Pearson's correlation analysis. The r-value of co-culture at 48 h is around 0.7. Considering the limitations of *in vitro* studies, this value is impressive at this condition.

The single cell types were also used to identify chemicals' potential sensitive types. Each of the three cell types plays a very important role in spermatogenesis. The spermatogenesis includes the process of Spermatogonia A cells differentiating into

spermatozoa. Sertoli cells support spermatogenesis both functionally and physically. Leydig cells secrete testosterone which can indirect regulate the process. Any toxicity on these three types of cells will eventually affect testis function. Single cell culture models can also help to elucidate the underlying mechanisms of toxicants to testes. For example, Leydig cell models were often used to investigate the chemicals' effect on steroidogenesis.

Cytotoxicity test was usually the first step of in *vitro* tests in replacement of animal studies [71]. The concentrations in cytotoxicity tests that can lead to non-specific alterations in cellular functions may cause effects on organ level and/or death of the organism [72]. NR dye uptake assay is one of the most sensitive and reliable cytotoxicity tests. It has been employed by Environmental Protection Agency to predict the starting dose of acute oral system toxicity and harmful tobacco smoke toxicants. Thus, in our system, we also used NR dye uptake assay to evaluate the toxicity of these chemicals. The co-culture can distinguish the toxicity of different chemicals, and more importantly, prioritize chemicals at high risk by cluster analysis. By doing NR uptake assay, the dose response curves of each chemical were acquired. It is not feasible to compare the different toxicities of chemicals using the response-curves because of the different concentration range for each chemical. Therefore, the inhibitory concentrations (IC) from 20% to 90% were calculated to indicate the toxicity of each chemical.

The inhibitory concentrations were then imported to non-supervised cluster analysis to distinguish different toxicities of chemicals. Three clusters were identified and defined as very toxic, medium toxic, and least toxic. After comparing with published *in vivo* studies, I found that our results were consistent with rat data. The rLOAEL values of Cd, ZEA, As, DES and HEP in rats were 0.088, 1, 8, 10, and 3 mg/kg/day, respectively, indicating their high toxicity to rats [65, 73]; they were defined as very toxic in our system. DEP, DOTP and DMP, which belong to the least toxic group, are well known as developmentally non-toxic phthalates [55, 74]. SAC is a sweetener and often used as a negative reference compound in embryo-toxicity tests; it was also not toxic in our model. Thus, cluster analysis can help to predict the toxicity levels of new chemicals based on the cluster the chemical resides in. The toxicity levels of different categories of chemicals were also assessed. For bisphenols, the order of toxicity was: TBBPA > BPAF > BPA > BPS. For pesticides, the order was: As > HEP > TCS > HEX > CHL > PARA > VIN > BA. For phthalates, the order was: DPP > DBP > BBP > DEHP > DMP, DEP, DOTP.

Different cell types displayed different sensitivities to the same chemical by treating each single cell type, as indicated by $IC_{50}$ values. In our system, Leydig cells were more sensitive to DPP, suggesting that DPP probably be an endocrine disruptor [75]. The $IC_{50}$ values of BPA, TCP and Cd for Sertoli cells were lower than for other cell types, indicating that Sertoli cells may be their targets. In literature, DPP is shown to be an anti-androgenic compound and reported to interfere with fetal testicular testosterone production in rats, suggesting its possible targets to be Leydig cells [76]. Cd and BPA were reported to induce testicular injury at the blood-testis barrier (Sertoli cells) to elicit subsequent damage to germ cells, and cause germ cell loss [77]. The primary targets of TCP in testes are Sertoli cells [78]. Thus, the results from treating single cell types may provide some hints regarding chemicals' targets *in vivo*.

The chemicals' toxicity was time-dependent. This was indicated by the higher R-values in Pearson correlation coefficient, and $R^2$ values in linear regression, at 48h than 24h. Chemicals were generally more toxic at 48 h than at 24 h for both co-culture and single cell types. We conclude that the treatment time greatly influences the toxicity of chemicals. In future studies, perhaps more time points could be tested to select the optimal treatment time. The best exposure time for each chemical would enable the prediction of plasma concentration in vivo where the toxicity occurs [79].

For chemicals with low toxicity, such as DEP, DMP and DOTP, the 50% decrease in cell viability requires very high doses, making it hard to achieve within the current dose range. Thus, IC10 or IC20 could be used to represent the toxicity of these chemicals. In our research, BMD were listed as another reference for chemicals' toxicity. BMD represents an exposure due to a dose of a substance associated with a specified low incidence of risk, generally in the range of 1% to 10%, of a health effect; or the dose associated with a specified measure or change of a biological effect.

By comparing the current model with our previous primary cells co-culture model, we found that both our cell line model and the primary co-culture model distinguished the toxic phthalates (DEHP, DBP, BBP and DPP) from the non-toxic phthalates (DEP, DMP and DOTP). The current cell line model induced higher cell death than previous primary cells model at the same concentrations for Cd treatment.

The reproductive toxicity of ME is reported *in vivo*, but without effect in our system. ME was reported to induce testicular atrophy and disruption of spermatogenesis via the metabolism of Ethylene glycol monomethyl ether (EGME) [84, 85]. It was found that a 4-week administration of ME at relatively low doses, corresponding to 0.08-0.325 mM/kg/day, was sufficient to produce marked testicular atrophy and a decrease in epididymis and prostate weights in a dose-dependent manner [86]. The possible reason may be the necessity of bio-activation for chemicals to induce their toxic effects [87]. It was found that ME undergoes metabolic activation to appropriate methoxyacetic acid (MAA) via EGME [88]. MAA primarily affects tissues with rapidly dividing cells and high rates of energy metabolism in testes, leading to apoptosis of primary spermatocytes. MAA is associated with changes in the expression of various genes and signaling pathways including oxidative stress in spermatocytes [89]. MAA was also reported to regulate the transcriptional activity of nuclear receptors including androgen receptor to contribute to the testicular toxicity [90]. Thus, the lack of effect of ME in our model may be due to lack of the complete metabolism *in vitro*. In the future experiments, MAA could be tested in our co-culture system to test its toxicity in our system.

A vitally important theme in reproductive toxicity studies is the assessment of *in vitro* and *in vivo* models that are predictive for adverse effects in humans exposed to chemicals. Our *in vitro* cell viability data were directly linked to rat rLOAEL. Thus, those chemicals toxic in our system may be toxic to rats. Considering that the prediction rate of animal studies to human toxicity is only 50% -70% [94, 95], there is a certain distance to correctly predict toxic chemicals in human. In order to predict the *in vivo* toxicities, the *in vitro* data has to be linked to human or animal plasma concentration, where the toxicity would occur. Other important factors including protein binding, metabolic stability, metabolic activation, metabolites, temporal relationship and compound solubility must also be addressed. Thus, it is unlikely that any individual *in vitro* model is sufficient as a final decision point for toxicity. A series of models which can provide a series of important information in a tiered approach is needed to improve the prediction of *in vitro* assays [79].

**In summary,** we obtained dose and time dependent data on cytotoxicity, cell viability, high throughput quantitative morphological data from Cellomics Image analysis for 32 compounds; and calculated the predictivity, precision, and accuracy for the compounds tested in this 3D-TCCS model. We evaluated the performance of our 3D-TCCS model for R/D toxicity, and compared these cytotoxicity and morphological data to *in vivo* results. these results provided essential dose and time dependent data to discriminate R/D toxicants.

**Specific Aim 3: To develop an integrated pathway-based high content (HCA) and high throughput (HTP) screening assay in the 3D-TCCS model for R/D toxicity evaluation.**

There is a need for improved *in vitro* methods to meet the challenges associated with the increasing push to predict the toxicity of chemicals. The Environmental Protection Agency (EPA) has initiated a ToxCast project integrating *in vitro* high-content and high-throughput toxicity assessment to characterize the toxicological profiles of thousands of chemicals [97-100]. High-content analysis (HCA) has been demonstrated to be particularly useful for toxicity testing and prediction as it enables measurements of multiple, early toxicological mechanisms by characterizing co-expression of multiple molecules, as well as quantification and visualization of the spatial and temporal dynamic processes of cellular events. HCA has been successfully applied to the prediction of drug-induced human hepatotoxicity, and this highly specific and sensitive assay has shown high concordance with human data [101-104]. Furthermore, the HCA enables comparisons of the effectiveness of various assay parameters, detects high-risk chemicals and the sequences of cellular events. By linking chemical-biological interactions with sequential key events at multiple biological responses, adverse outcome pathways provide a mechanism-based framework to support the hazard assessment of chemicals [105, 106]. The purpose of this study was to develop an automated multi-parametric screening method and to optimize protocols for cell treatment, high-content imaging, and image analysis of the C18-4 spermatogonial cells. We applied this validated HCA approach to characterize and compare the testicular toxicities of BPA and three selected commercially available BPA analogues: bisphenol S (BPS), bisphenol AF (BPAF) and tetrabromobisphenol A (TBBPA). We concurrently compared a wide spectrum of cellular and molecular events that potentially lead to impaired male reproductive function, including nuclear morphology, DNA content,

Fig. 5. High-Content, High-Throughput Analysis in in vitro “mini-testis” model

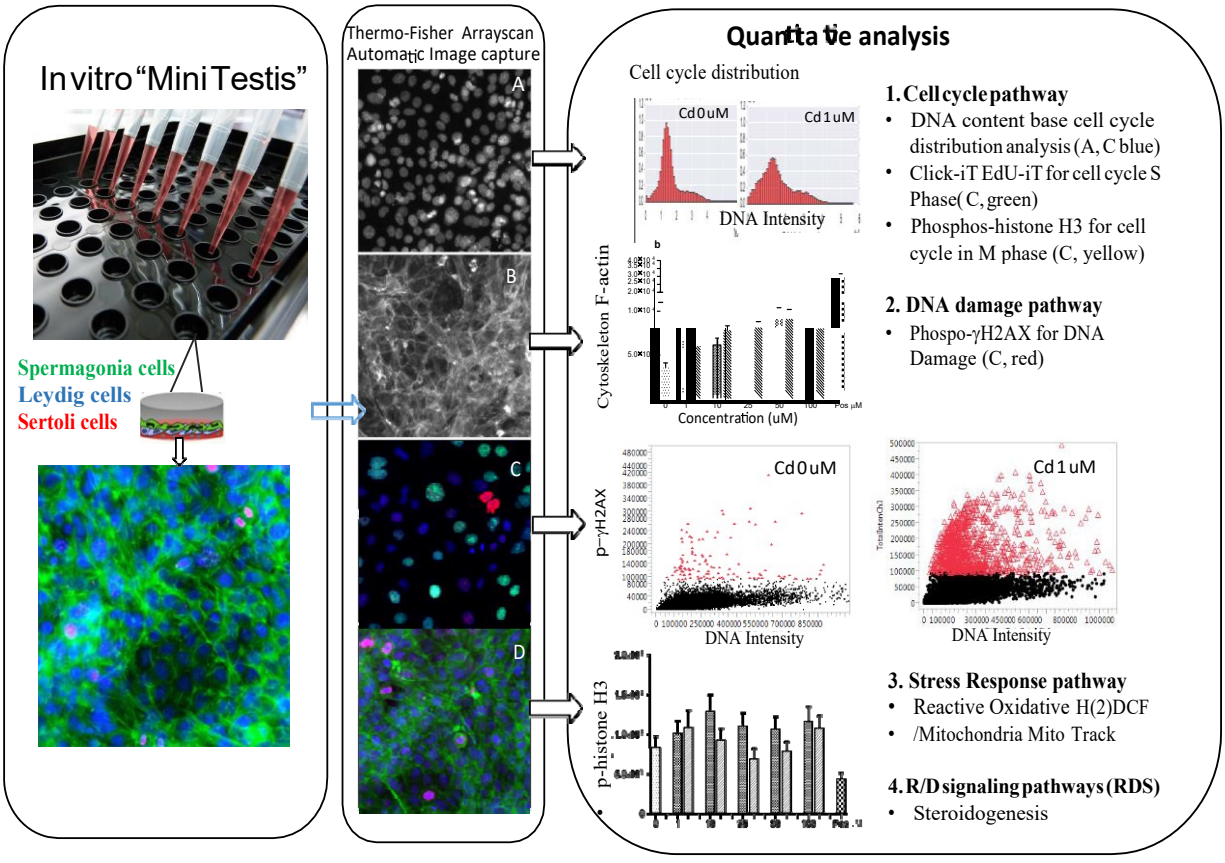

cytoskeletal integrity, cell cycle, and DNA damage responses in a dose and time-dependent manner (Figure 5). Overall, our results demonstrated that this *in vitro* model combined with HCA can be utilized for a quantitative screening of chemical effects in spermatogonial cells and enable rapid and cost-effective measurement of the multidimensional biological profile of toxicity.

**Cell culture and treatment**

The mouse C18-4 spermatogonial cell line was established from germ cells isolated from the testes of 6-day-old Balb/c mice. This cell line shows morphological features of type A spermatogonia, expresses germ cell–specific genes such as GFRA1, Dazl and Ret, which are markers specific for germ cells in the testis [56, 57]. Cells were maintained in DMEM medium composed of 5% FBS, and 100 U/ml streptomycin and penicillin in a 33˚C, 5% $CO_2$ humidified environment in a sub-confluent condition with passaging every 3-4 days. When they reached 70-80% confluence, cells were inoculated with $1.2 \times 10^4$ per well in a 96-well plate. Cells were cultured overnight and treated with various concentrations of BPA, BPS, BPAF and TBBPA for the indicated doses and time periods.

**Cell viability**

Cell viability was determined by measuring the capacity of cells to take up NR. NR can be retained inside the lysosomes of viable cells, while the dye cannot be retained if the cells dies. Dye retention is proportional to the number of viable cells, and can be measured based on NR absorbance [63, 64]. Significant changes in cell viability were determined using a one-way analysis of variance (one-way ANOVA) followed by Tukey-Kramer multiple comparison tests. Briefly, cells were treated with various concentrations of BPA, or BPS, (50, 100, 200 and 400 μM), and BPAF or TBBPA (25, 50, 75 and 100 μM) for different length of time (24-72 h). Cells treated with vehicle (0.05% DMSO) were used as the reference group with cell viability set as 100%. After treatments, the culture medium was removed and fresh medium containing NR (50 μg/ml) was added. Following 3 h incubation, cells were washed with phosphate buffered saline (PBS) and NR was eluted with 100 μl of a 0.5% acetic acid/50% ethanol solution. The plate was gently rocking on a plate shaker, and absorbance values was measured at 540 nm with a Synergy HT microplate reader (BioTek, VT). Cell viability was expressed as percentage of the mean of vehicle controls after subtracting the background control.

**Fluorescence staining and image acquisition**

For cell cycle analysis, cells were incubated with BrdU (40 μM) for 3 h prior to fixation. Cells in the controls reached 100% confluence at the time of harvest. Cells were then fixed with 4% paraformaldehyde for 30 mins at room temperature, followed by three times washing with PBS. Cells were then acidified with a 4N HCl/ Triton X-100 solution for 30 min at room temperature. After neutralization with $Na_2B_4O_7$ solution for 10 min, cells were washed twice with PBS, and blocked with 3% BSA in PBS. Cells were then incubated with a mouse anti-BrdU antibody (Thermo Scientific, MA) in PBS/BSA/0.5% Tween 20 overnight at 4°C. After washing twice with PBS/BSA, cells were incubated with a goat anti-mouse DyLight 488 and the DNA staining dye Hoechst 33342 (Thermo Scientific, MA) in PBS/BSA solution for 90 min at room temperature.

For DNA damage responses and cytoskeleton analysis, cells treatments and fixation were the same as described above. After fixation, cells were permeabilized by 0.1% Triton X-100 in PBS, then incubated with mouse anti-phospho-Histone-H2AX (Ser139) (γ-H2AX)

(Millipore, MA) in PBS/BSA/0.5% Tween 20 solution overnight at 4°C. After washing twice with PBS/BSA, cells were incubated with goat anti-mouse Dylight 650 (Thermo Scientific, MA), and Hoechst 33342 in PBS/BSA solution for 90 min at room temperature. Prior to image acquisition, cells were stained with Alexa Fluor 488 Phalloidin (Cell Signaling, MA) for F-actin staining for 30 min at room temperature.

Multichannel images were automatically acquired using an Arrayscan™ VTI HCS reader with HCS Studio™ 2.0 Target Activation BioApplication module (Thermo Scientific, MA). Forty-nine fields per well were acquired at 20x magnification using Hamamatsu ROCA-ER digital camera in combination with 0.63x coupler and Carl Zeiss microscope optics in auto-focus mode. Channel one (Ch1) applied the BGRFR 386_23 for Hoechst 33342 that was used for auto-focus, object identification and segmentation. Image smoothing was applied to reduce object fragmentation prior to object detection in Ch1. Border objects were excluded. For BrdU staining, channel two (Ch2) applied the BGRFR 549_15 for BrdU. For F-actin and γ-H2AX staining, Ch2 applied the BGRFR 485_20 for F-actin and channel three (Ch3) applied the BGRFR 650_13 for γ-H2AX.

**High-content images analysis**

Multi-Channel images were analyzed using HCS Studio™ 2.0 TargetActivation BioApplication. Change in nuclear morphology is an early event of the cellular response, and is associated with cellular function [107-109]. Single-cell based HCA provided multiple parameters to characterize the nucleus, including the number, nuclear area, shape, and total or average intensity. Nuclear shape measurement included P2A and LWR parameters. P2A is a shape measurement based on the ratio of the nuclear perimeter squared to 4π*nucleus area (perimeter$^2$/4 π * nucleus area), which evaluates nucleus smoothness. LWR (length-width ratio) measures the ratio of the length to the width of the nucleus, which evaluates nucleus roundness. For a fairly round and smooth object, the values for P2A and LWR are around 1.0. Total intensity was defined as total pixel intensities within a cell in the respective channel; the average intensity was defined as the total pixel intensities divided by the area of a cell in the respective channel. With 49 fields of each well, at least 5000 cells were analyzed per well and single-cell based data for each channel were exported for further statistical analysis. The experiments were performed with at least three biological replicates and repeated twice.

HCA-based cell cycle analysis was conducted as recently reported by Roukos et al [110]. The frequency distributions of total DNA intensity of all individual nuclei were calculated and plotted for each experimental condition in a custom script written in Python 3.5.2 (Python Software Foundation, OR; this script is freely available from the authors upon request). Cell cycle profiles with discrete sub-G1 (apoptotic cells), G0/1, S or G2/M populations in the controls and treatments were determined by the selections of appropriate thresholds of these gates as reported [110].

**Statistical Analysis**

All data obtained from the HCS Studio™ 2.0 TargetActivation BioApplication were exported and further analysis was conducted using the JMP statistical analysis package (SAS Institute, NC). Objects with nuclear area less than 50 μM$^2$ or larger than 800 μM$^2$ were excluded in order to remove cell debris and clumps. For each plate, the vehicle control showed consistent measurement for all endpoints tested. For intra-plate normalization, each sample value was normalized to the overall scaling factors, which was the mean of median values of vehicle control (0.05% DMSO) in each plate. The parameters from single-cell based imaging were quantified, and averaged for each well condition. For the mega or multi-nuclei

identification in the automatic HCA, nuclei with enlarged nuclear area (≥ 500 μm$^2$) and irregular nuclear shape (P2A ≥ 1.35) were identified, and the percentages were calculated. BrdU positive cells were set by the total intensity of BrdU in the control over 20,000 pixels. γ-H2AX positive cells were set by the total intensity of γ-H2AX in the control over 120,000 pixels. Data were presented as mean ± standard deviation (SD). Statistical significance was determined using one-way ANOVA followed by Tukey-Kramer all pairs comparison. A P value less than 0.05 denoted a significant difference compared to the vehicle control (*). To examine the relationship between the cytoskeleton and DNA damage responses, Spearman correlation analysis was conducted between log-transformed total intensity of F-actin and log-transformed total intensity of γ-H2AX at 24, 48 and 72 h. The 20% maximal effect concentration (EC20) and median lethal concentration (LC50) were calculated with a curve-fitting program using GraphPad Prism 5 (San Diego, CA). A dose-response curve fit was established based on the concentrations of chemicals that had a significant effect. The four-parameter nonlinear regression curve fit was applied. Treatment concentrations were $\log_{10}$ transformed. For cell viability (NR assay) and cell number data (HCA), the lowest value was set to be 0% and the highest value was set to be 100%. For other markers, the lowest value was set to be controls and the highest value was set to be a maximal effect at each time point.

**Results and Outcomes:**

**BPA and its analogues induced differential dose- and time-dependent cytotoxicity in spermatogonial cells**

In order to select sub-lethal doses of BPA and its analogues for HCA analysis in spermatogonial cells, cell viability was measured using NR uptake assay. Figure 6 shows significant dose- and time-dependent decreases of cell viability in spermatogonial cells treated with BPA and its analogues for 24 h and 48 h. BPAF reduced cell viability starting at a concentration of 25 μM, TBBPA reduced cell viability starting at a dose of 50 μM for 24 h and 25 μM for 48 h, while BPA and BPS reduced cell viability at a concentration of 100 μM for both 24 and 48 h exposure. This indicated that BPAF and TBBPA induced greater cytotoxicities, as compared to BPA and BPS. The LC50 values for 48 h were 42.16, 49.93, 132.7, 325.3 μM for BPAF, TBBPA, BPA and BPS, respectively. The highest concentrations of 50 μM were selected for BPA and BPS, and 25 μM were selected for BPAF and TBBPA in the following HCA experiments.

Figure 6. Cell viability was determined by neutral red uptake assay in C18-4 spermatogonial cells treated with BPA, BPS and BPAF.

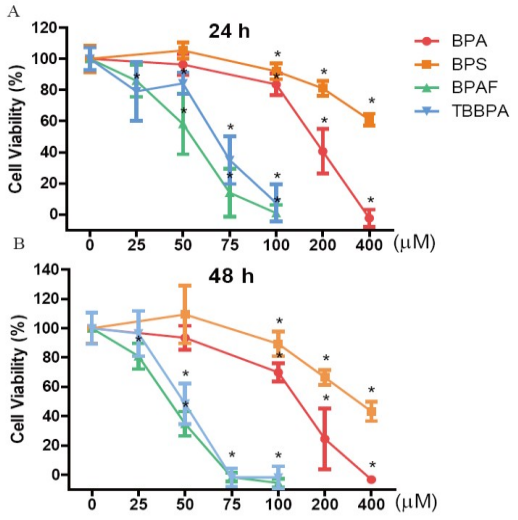


**BPA and its analogues altered nuclear morphology and cell number**

Nuclear morphology has shown to be a sensitive endpoint compared to conventional cytotoxicity assays [111]. In this study, we measured multiple parameters associated with nuclear morphology. Figure 7A shows representative nuclear morphologies following 72 h treatments. Notable reductions of cell numbers and increases of mega or multinucleated cell numbers were observed in the BPAF treatments at doses of 10 and 25 μM (arrows). Further

quantification of the multinucleated cells using HCA demonstrated that BPAF treatment induced significant increases of multinucleated cells at doses of 25 μM for 24, 48 and 72 h. No obvious morphological change was observed for the other tested compounds. As shown in Figure 7B-D, nuclear morphological parameters obtained from HCA, including nuclear area and nuclear shape, were compared in spermatogonial cells treated with various chemicals for 24, 48 and 72 h. Significant increases of nuclear area were observed in cells treated with 25 μM BPAF for 24, 48 and 72 h, and cells treated with 50 μM BPS and 25 μM TBBPA for 72 h. BPA significantly decreased LWR at a dose of 50 μM for 72 h. BPS significantly decreased LWR and P2A at a dose of 50 μM for 72 h. However, BPAF significantly increased LWR and P2A at concentrations of 25 μM for 24 h, 10 μM for 48 h. For 72 h, BPAF significantly increased LWR at 1 μM and P2A at 10 μM. TBBPA also induced significant increases of LWR at concentrations of 5, 10 and 25 μM and a significant increase of P2A at a concentration of 25 μM for 72 h.

Figure 7. High-content analysis of nuclear morphology of C18-4 spermatogonial cells treated with BPA, BPS, BPAF and TBBPA. A shows the representative images (40x) of controls and cells treated with BPA and BPS (1, 10 and 50 μM), BPAF and TBBPA (1, 10 and 25 μM) for 72 h. Arrows indicate the multinucleated cells. Scale bar = 50 μm. B-D shows the quantification of absolute nuclear area (μm²), nuclear shape, including LWR for nuclear roundness and P2A for smoothness.

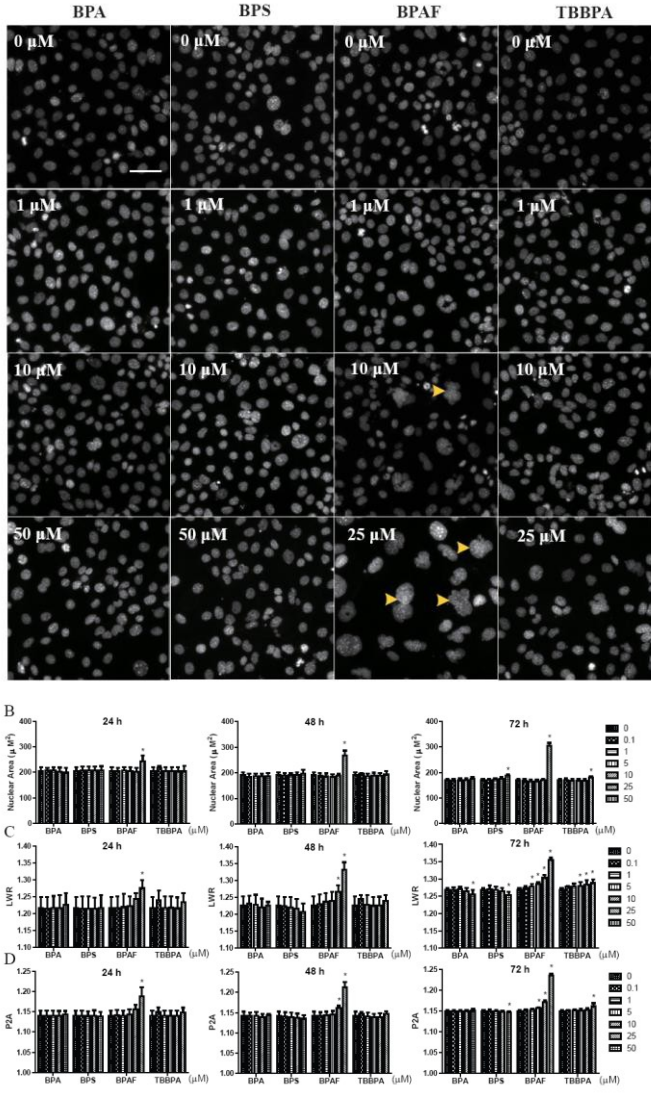


Figure 8. High-content analysis of DNA content and synthesis of the spermatogonial cells treated with BPA, BPS, BPAF and TBBPA. The nuclei were stained with Hoechst 33342. Cells were incubated with 5-bromo-2'-deoxyuridine (BrdU, 40 μM) for 3 h prior to cell fixation, and then stained with mouse anti-BrdU antibody and anti-mouse DyLight 488 for detection of BrdU incorporation (green).

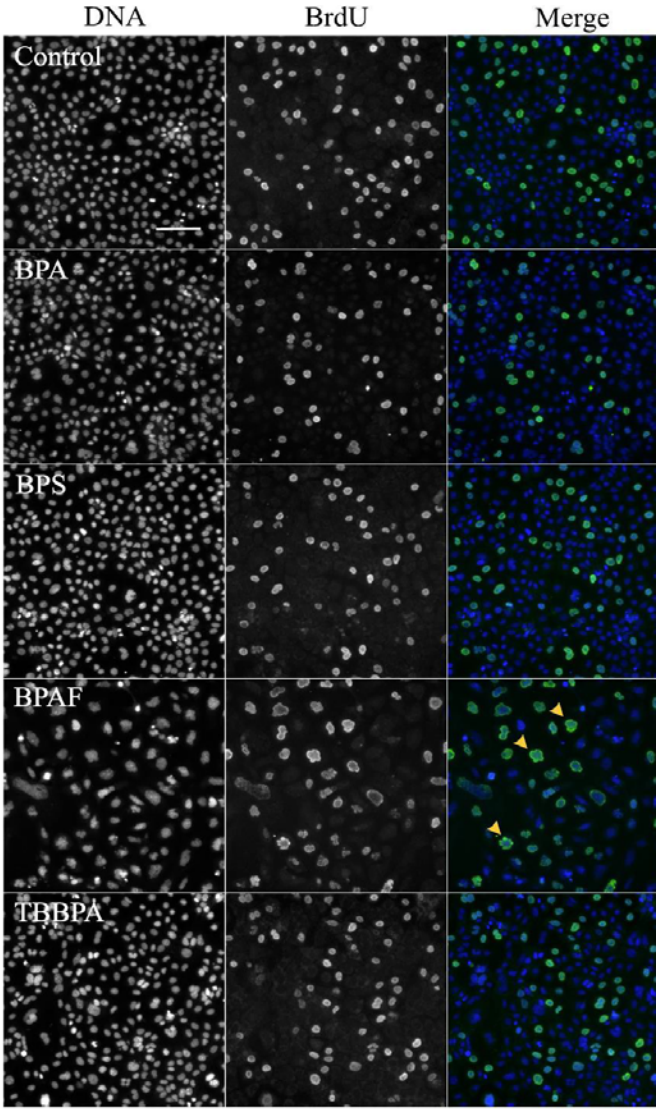

Figure 8B-D

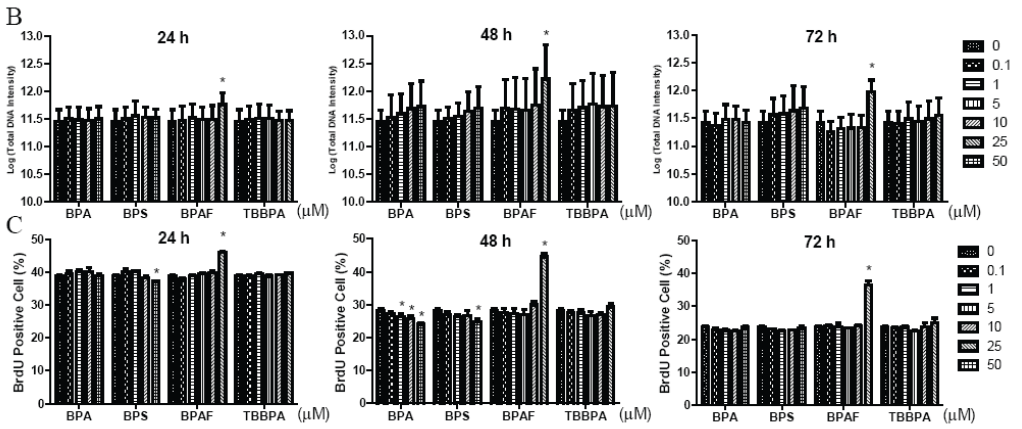


BPAF and TBBPA reduced cell numbers starting at a dose of 25 μM for 24, 48 and 72 h. BPA and BPS reduced cell numbers at a dose of 50 μM for 24, 48 and 72 h. These numbers were lower than those observed with the NR assay. Notably, low doses of BPA (0.1 μM) and BPAF (0.1 and 5 μM) slightly increased cell numbers. These results suggested that for the detection of changes in cell numbers measured by HCA is more sensitive than the conventional NR uptake cytotoxicity assay.

**BPA and its analogues affected DNA synthesis and cell cycle**

The measurement of DNA content of individual cells enabled determination of the phases of the cell cycle, while the BrdU incorporation measured newly synthesized DNA. Figure 8A shows representative images of BrdU incorporation after 72 h treatments. Most multinucleated cells in the BPAF treatment were BrdU positive cells. As shown in Figure 8B, BPAF (25 μM) significantly induced total DNA intensity, by 1.3-, 1.5- and 2.0-fold after 24, 48 and 72 h treatments as compared to the control, respectively. However, BPA, BPS, and TBBPA treatments shows no observable change of DNA total intensity. Figure 8C showed that BPS of a concentration of 50 μM and BPA of concentrations of 10, 25, 50 μM significantly decreased BrdU positive cells for 24 and 48 h, respectively, suggesting inhibitory effects of DNA synthesis from those treatments. However, BPAF treatment induced significant increases in BrdU positive cells at all three time-points at a concentration of 25 μM as compared to the control. No change of BrdU incorporation was observed for the TBBPA treatment.

Figure 9. High–content analysis of cell cycle of spermatogonial cells treated with BPA, BPS, BPAF and TBBPA.

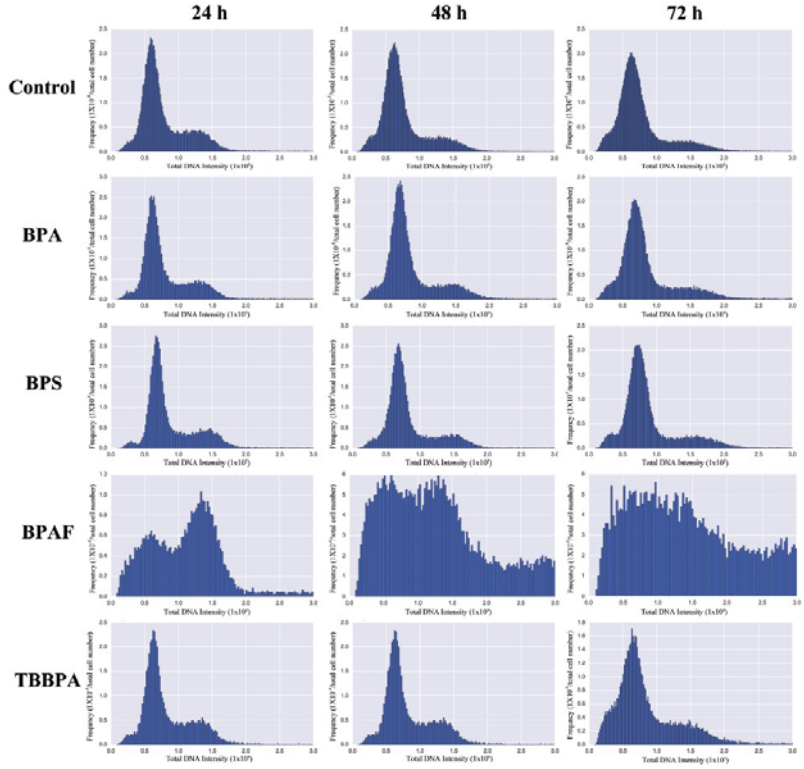


Histogram plots of total

DNA intensity were generated and the percentages of cells in each phase of the cell cycle were determined. As shown in Figure 9, the DNA intensity histogram in control groups exhibited distinguishable 2N (G0/1 phase) and 4N DNA (G2/M phase) peaks. Significant changes in the DNA histogram plot such as decreases of G0/1, and increases of S and G2/M phases in the BPAF treatment were observed. As shown in Table 4, dynamic changes of cell cycle stages in the controls across time-points, such as increases of cells in G0/1 and decreases of cells in S phase after 48 and 72 h culture were observed as compared to the control after 24 h. Cell populations in G0/1 phase were significantly decreased with a BPAF treatment of 25 μM for 24 h, 10, 25 μM for 48 and 72 h, and a TBBPA treatment of 25 μM for 24, 48 and 72 h. Significant increases of the percentage of cells in S phase were observed

TABLE 4. HCA of Cell Cycle of Spermatogonial Cells Treated with Various Concentrations of BPA, BPS, and BPAF, TBBPA for 24, 48, and 72 h

| | Dose (μM) | 24 h | | | | 48 h | | | | 72 h | | | |
|---|---|---|---|---|---|---|---|---|---|---|---|---|---|
| | | Sub G1(%)[a] | G0/1(%) | S (%) | G2/M (%) | Sub G1(%)[a] | G0/1(%) | S (%) | G2/M (%) | Sub G1(%)[a] | G0/1(%) | (%)S | G2/M (%) |
| BPA | 0 | 3.5 ± 1.1 | 64.6 ± 1.7 | 12.6 ± 0.8 | 18.1 ± 1.7 | 5.2 ± 1.5 | 67.4 ± 1.6 | 12.0 ± 0.7 | 13.0 ± 1.1 | 5.6 ± 1.0 | 70.7 ± 1.7 | 9.9 ± 1.4 | 12.9 ± 1.0 |
| | 0.1 | 3.5 ± 0.9 | 64.9 ± 1.5 | 12.6 ± 0.2 | 18.1 ± 1.1 | 5.2 ± 3.1 | 69.4 ± 2.3 | 12.4 ± 0.7 | 12.5 ± 2.8 | 6.9 ± 1.2 | 70.0 ± 0.8 | 10.6 ± 0.6 | 11.7 ± 1.3 |
| | 1 | 4.4 ± 2.1 | 62.5 ± 1.5 | 12.9 ± 0.8 | 18.9 ± 1.9 | 5.9 ± 1.5 | 67.9 ± 1.2 | 12.1 ± 0.6 | 13.6 ± 1.8 | 6.5 ± 1.1 | 70.7 ± 2.1 | 9.3 ± 2.1 | 12.2 ± 1.0 |
| | 10 | 5.0 ± 1.3 | 64.0 ± 1.0 | 11.8 ± 0.9 | 18.3 ± 1.3 | 4.7 ± 1.4 | 67.0 ± 2.2 | 11.7 ± 1.4 | 15.7 ± 1.2* | 6.8 ± 0.6 | 70.6 ± 3.1 | 11.3 ± 2.6 | 9.8 ± 1.2* |
| | 50 | 4 ± 1.3 | 65.8 ± 3.0 | 13.5 ± 0.6 | 15.3 ± 1.3* | 4.2 ± 1.7 | 67.1 ± 1.9 | 12.9 ± 0.8 | 15.1 ± 1.6 | 7.3 ± 1.3* | 67.5 ± 3.1 | 11.0 ± 1.7 | 13.1 ± 1.9 |
| BPS | 0 | 3.5 ± 1.1 | 64.6 ± 1.7 | 12.6 ± 0.8 | 18.1 ± 1.7 | 5.2 ± 1.5 | 67.4 ± 1.6 | 12.0 ± 0.7 | 13.0 ± 1.1 | 5.6 ± 1.0 | 70.7 ± 1.7 | 9.9 ± 1.4 | 12.9 ± 1 |
| | 0.1 | 3.8 ± 0.8 | 63.6 ± 1.5 | 12.3 ± 0.2 | 19.4 ± 2.0 | 4.3 ± 0.6 | 69.5 ± 1.1 | 11.8 ± 0.7 | 13.7 ± 1.8 | 7.4 ± 1.7 | 71.0 ± 1.1 | 9.5 ± 1.3 | 11.4 ± 0.8 |
| | 1 | 3.6 ± 0.7 | 62.9 ± 2.0 | 12.6 ± 0.5 | 20.0 ± 1.1 | 3.7 ± 1.8 | 68.4 ± 1.8 | 11.7 ± 0.5 | 15.0 ± 1.6 | 6.5 ± 0.6 | 71.9 ± 1.8 | 9.6 ± 1.4 | 11.3 ± 1.1 |
| | 10 | 3.8 ± 0.9 | 63.1 ± 1.9 | 12.9 ± 0.7 | 19.2 ± 1.3 | 4.9 ± 1.3 | 66.6 ± 1.2 | 11.9 ± 0.9 | 15.6 ± 2.3* | 8.7 ± 5.0 | 70.1 ± 1.9 | 10.2 ± 1.5 | 10.2 ± 2.8* |
| | 50 | 3.9 ± 1.1 | 63.7 ± 1.3 | 13.0 ± 0.8 | 18.6 ± 1.6 | 5.9 ± 3.4 | 65.9 ± 2.5 | 11.2 ± 0.9 | 16.0 ± 1.9* | 7.4 ± 1.4 | 70.5 ± 2.5 | 9.2 ± 1.6 | 11.8 ± 2.6 |
| BPAF | 0 | 3.5 ± 1.1 | 64.6 ± 1.7 | 12.6 ± 0.8 | 18.1 ± 1.7 | 5.2 ± 1.5 | 67.4 ± 1.6 | 12.0 ± 0.7 | 13.0 ± 1.1 | 5.6 ± 1.0 | 70.7 ± 1.7 | 9.9 ± 1.4 | 12.9 ± 1.0 |
| | 0.1 | 3.6 ± 1.0 | 64.3 ± 1.9 | 11.9 ± 1.0 | 18.5 ± 1.3 | 5.6 ± 1.9 | 66.5 ± 2.2 | 10.6 ± 0.4 | 16.6 ± 1.4 | 6.5 ± 0.7 | 71.5 ± 1.0 | 10.4 ± 0.5 | 11.1 ± 1.1 |
| | 1 | 3.3 ± 0.7 | 65.1 ± 1.4 | 13.5 ± 0.5 | 17.3 ± 2.0 | 5.4 ± 1.4 | 68.1 ± 2.0 | 11.5 ± 1.4 | 14.0 ± 2.1 | 7.7 ± 1.1 | 67.9 ± 3.3 | 10.9 ± 1.1 | 12.8 ± 1.2 |
| | 5 | 4.1 ± 1.0 | 63.5 ± 2.8 | 12.1 ± 0.7 | 18.7 ± 1.5 | 5.5 ± 2.0 | 67.8 ± 3.5 | 11.6 ± 1.3 | 14.1 ± 4.2 | 8.0 ± 0.7* | 70.0 ± 1.0 | 10.3 ± 1.2 | 11.2 ± 1.1 |
| | 10 | 6.1 ± 1.6* | 62.2 ± 1.8 | 12.3 ± 0.8 | 18.5 ± 1.2 | 8.4 ± 4.1 | 59.7 ± 1.5* | 11.0 ± 0.6 | 19.9 ± 3.2* | 12.1 ± 2.5* | 61.0 ± 1.3* | 13.1 ± 2.1* | 13.1 ± 1.1 |
| | 25 | 7.6 ± 1.9* | 25.3 ± 3.3* | 14.9 ± 1.6* | 47.6 ± 4.6* | 9.7 ± 1.7* | 25.3 ± 3.1* | 15.2 ± 1.4* | 44.6 ± 2.7* | 6.8 ± 2.5 | 26.4 ± 3.0* | 19.3 ± 1.3* | 48.3 ± 5.1* |
| TBBPA | 0 | 3.5 ± 1.1 | 64.6 ± 1.7 | 12.6 ± 0.8 | 18.1 ± 1.7 | 5.2 ± 1.5 | 67.4 ± 1.6 | 12.0 ± 0.7 | 13.0 ± 1.1 | 5.6 ± 1.0 | 70.7 ± 1.7 | 9.9 ± 1.4 | 12.9 ± 1.0 |
| | 0.1 | 4.9 ± 2.0 | 62.4 ± 1.7 | 12.9 ± 0.7 | 19.1 ± 2.0 | 4.1 ± 1.9 | 69.1 ± 1.9 | 11.4 ± 0.4 | 14.8 ± 3.3 | 7.4 ± 1.2 | 71.0 ± 0.5 | 10.3 ± 0.4 | 10.8 ± 0.9 |
| | 1 | 3.7 ± 1.0 | 62.7 ± 1.0 | 13.3 ± 0.8 | 19.6 ± 1.1 | 5.4 ± 1.4 | 66.7 ± 2.8 | 12.0 ± 0.8 | 15.0 ± 2.9 | 8.6 ± 0.9 | 69.4 ± 0.7 | 10.5 ± 0.5 | 10.6 ± 0.7 |
| | 5 | 4.3 ± 1.5 | 62.9 ± 1.7 | 13.2 ± 0.7 | 18.7 ± 0.9 | 3.4 ± 1.1 | 67.6 ± 1.6 | 11.9 ± 0.6 | 16.3 ± 2.0* | 8.6 ± 4.5 | 69.7 ± 3.7 | 9.9 ± 0.4 | 11.2 ± 0.7 |
| | 10 | 4.2 ± 1.5 | 66.3 ± 1.7 | 11.0 ± 1.1* | 18.0 ± 2.1 | 5.5 ± 1.7 | 66.5 ± 1.6 | 8.9 ± 2.3* | 18.1 ± 1.4* | 11.0 ± 2.0* | 67.7 ± 1.6 | 6.7 ± 0.6* | 13.8 ± 1.0 |
| | 25 | 4.7 ± 1.0 | 60.3 ± 0.9* | 10.6 ± 1.2* | 23.5 ± 0.9* | 8.9 ± 3.6* | 63.2 ± 3.3* | 9.2 ± 1.3* | 17.7 ± 2.0* | 13.2 ± 2.3* | 57.5 ± 8.0* | 8.7 ± 1.1 | 19.1 ± 4.9* |

Note: Percentage of each stage of cell cycle, including sub-G1, G0/1, S and G2/M phase are presented as mean ± SD, $n = 6$. Three replicates in 2 separate experiments were included. Statistical analysis was conducted by 1-way ANOVA followed by Tukey-Kramer multiple comparison (*$P < .05$). Cells treated with vehicle (0.05% DMSO) were used as negative controls (0).

[a]Cells with DNA content less than 2N, representing apoptotic cells.

when cells were treated with 25 μM BPAF for 24, 48 h, and 10, 25 μM for 72 h. On the contrary, significant decreases in the percentage of cells in S phase were observed after treatments with 10 and 25 μM TBBPA for 24 and 48 h, and after treatment with 10 μM for 72 h. Accumulations of cells in G2/M phase were observed in cells treated with 10 μM BPA for 48 h, and 10 and 50 μM BPS for 48 h. A similar pattern was observed with 25 μM BPAF for 24 h, 10 and 25 μM BPAF for 48 h, and 25 μM BPAF for 72 h. Accumulations of cells in G2/M were also observed with 25 μM TBBPA for 24 and 72 h, and with doses of 5, 10 and 25 μM of TBBPA for 48 h. Significant decreases in the percentages of cells in G2/M phase were observed with a BPA treatment of 50 μM for 24 h and of 10 μM for 72 h. A BPS treatment of 10 μM for 72 h had the same effect. Finally, increases in the percentages of cells in sub-G1 phase, representing apoptotic cells, were observed with BPA at a dose of 50 μM for 72 h, with BPAF treatment at doses of 10 and 25 μM for 24 h, 25 μM for 48 h, 5and 10 μM for 72 h. TBBPA treatments of25

μM for 48 h, and of 10, 25 μM for 72 h also increased the percentages of cells in apoptosis. Altogether, these results indicated that BPAF and TBBPA treatments at higher concentrations led to an increase of cells in the G2/M phase accompanied by an increase of apoptotic cells. Further, BPAF treatment showed unique increase of cells in S phase, which was consistent with our BrdU incorporation results. On the contrary, BPA and BPS treatments led to a decrease in the number of cells in the G2/M phase at doses of 10 or 50 μM.

**BPA and its analogues disrupted the germ cell cytoskeleton**

The cytoskeleton provides a structural framework for the cell and serves as a scaffold that determines cell shape and the organization of the cytoplasm [112]. We developed multi-parametric HCA assays to examine the effects of BPA and its analogues on the cytoskeleton of the spermatogonial cells. As shown in Figure 10A, F-actin showed a regular organization with aligned and tightly compacted structures in controls. However, BPAF and TBBPA treatments induced actin aggregate as dot-like structures with highly condensed actin staining (arrows). We further quantified the number of dot-like structures of F-actin and found significant increases in BPAF treatment at doses of 25 μM for 24, 48 and 72 h, and TBBPA treatment at doses of 25 μM for 24 and 48 h. Significant decreases of dot-like structures were observed in BPS treatment of 50 μM for 72 h. These unique structure changes were dose-dependently observed for the of BPAF and TBBPA treatments, suggesting chemical-specific effects on the cytoskeleton. Dynamic changes of total intensity of F-actin were further quantified as shown in Figure 10B. BPA and BPS (50 μM), BPAF and TBBPA (25 μM) significantly increased total intensity of F-actin at 24, 48 and 72 h exposure times. BPAF induced an approximate 2-fold increase of total F-actin intensity at 48 and 72 h exposure in comparison with other bisphenols. These data suggested that BPAF and TBBPA could potentially impair F-actin polymerization, resulting in aberrant F-actin accumulation.

**BPA and its analogues induced γ-H2AX expression, a marker for early DNA damage**

To further explore the potential effects of BPA and its analogues on DNA integrity, we examined γ-H2AX expression to assess early DNA damage responses in spermatogonial cells after treatments with BPA and its analogues. As shown in Figure 10A, all tested compounds induced various extent of γ-H2AX staining. BPAF induced γ-H2AX positive cells at a concentration of 25 μM. For the quantification of γ-H2AX as shown in Figure 10C, BPA treatment significantly increased the number of γ-H2AX positive cells at a concentration of 50 μM for 48 and 72 h. Both BPS (50 μM) and BPAF (25 μM) treatments significantly increased the number of γ-H2AX positive cells after 24, 48 and 72 h exposure, as compared to the control. TBBPA only induced γ-H2AX positive cells at a concentration of 25 μM for 72 h. BPAF induced a higher number of γ-H2AX positive cells, with increase of 2.5-, 3- and 5-fold for exposures of 24, 48 and 72 h respectively as compared to the control. These data demonstrated that BPAF showed greater genotoxic potency as observed by increased expression of the DNA damage response marker γ-H2AX.

Figure 10. High-content analysis of F-actin and γ-H2AX in spermatogonial cells treated with BPA, BPS, BPAF, and TBBPA. Arrows indicate dot-like structures. Scale bar = 100 μm. B-C demonstrated the quantification of log-transformed total intensity of F-actin and positive c-H2AX cells.

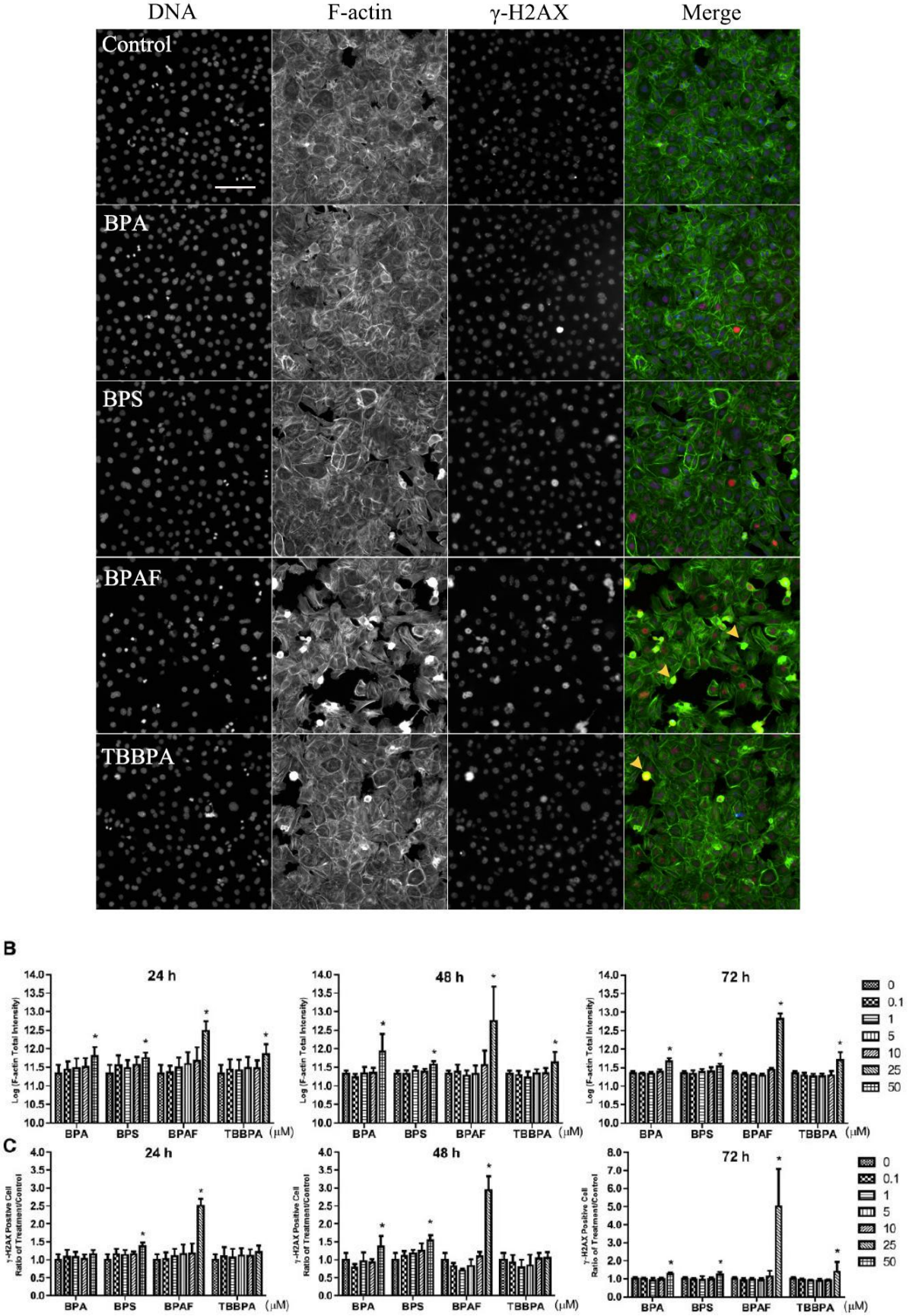

To examine the relationship between the cytoskeleton and DNA damage responses, a spearman correlation analysis was conducted based on log-transformed total intensity of F-actin and γ-H2AX. The correlation coefficients (r) are summarized in Table 5. For all four chemicals tested, r was positive with P values of less than 0.0001, suggesting a significant and positive correlation between cytoskeleton perturbation and DNA damage responses. Thus, an increase in the intensity of F-actin staining was strongly correlated with an increase in total intensity of γ-H2AX for 24 and 48 h exposure, and moderately correlated an increase in the total intensity of γ-H2AX for 72 h, suggesting that cytoskeleton perturbation may co-occur with the DNA damage responses.

TABLE 5. Correlation Analysis Between Total Intensity of F-actin and Total Intensity of c-H2AX

| | Correlation Coefficient | | | | | | | | | |
|---|---|---|---|---|---|---|---|---|---|---|
| Time (h) | BPA | | BPS | | BPAF | | TBBPA | | All | |
| | *r* | *P* | *r* | *P* | *r* | *P* | *r* | *P* | *r* | *P* |
| 24 | 0.85 | <.0001 | 0.91 | <.0001 | 0.45 | .0384 | 0.75 | <.0001 | 0.76 | <.0001 |
| 48 | 0.82 | <.0001 | 0.89 | <.0001 | 0.74 | .0001 | 0.34 | .1295 | 0.75 | <.0001 |
| 72 | 0.42 | .0827 | 0.66 | .0027 | 0.48 | .0276 | 0.52 | .0152 | 0.50 | <.0001 |

Note: Spearman correlation analysis was conducted between the log-transformed total intensity of F-actin and γ-H2AX in each cell (JMP statistical analysis package, SAS Institute, Cary, North Carolina).

**Comparison of EC20 values of BPA and its selected analogues for different endpoints**

In order to clarify the relationship between doses of compounds, the magnitude, and type of cellular responses (endpoints), the EC20 values from different endpoints were calculated and are listed in Table 3. Similar to cell viability data obtained with the NR assay, the EC20 values of multiple endpoints obtained with the HCA were lower in all treatments, suggesting HCA-based assays identify potential targets of cytotoxic agents with improved sensitivity. In BPA treatment, the endpoint with the lowest EC20 was cytoskeleton perturbation (7.5 μM), followed by cell number decrease (52.4 μM) and G2/M phase decrease (54.6 μM) after 24 h treatment. After 48 h treatment, the endpoint with the lowest EC20 was cytoskeleton

TABLE 6. EC20 Values of BPA and Its Selected Analogues from Multiple Endpoints

| | | 24 h | | | | 48 h | | | | 72 h | | | |
|---|---|---|---|---|---|---|---|---|---|---|---|---|---|
| | Dose (μM) | BPA | BPS | BPAF | TBBPA | BPA | BPS | BPAF | TBBPA | BPA | BPS | BPAF | TBBPA |
| Cell Viability [a] | $EC_{20}$ | 114.5 | 4222.1 | 11.5 | 41.7 | 84 | 154.3 | 10.1 | 47.1 | ND | | | |
| | CI | 101.1–129.6 | 198.6–248.3 | 3.9–33.4 | 31.5–55.2 | 72.8–97.0 | 123.1–193.4 | 39.6–25.7 | VW | | | | |
| Cell Number | $EC_{20}$ | 52.4 | 246.1 | 13.3 | 27.8 | 50 | 81.4 | 13.9 | 28.1 | 52.5 | 64.8 | 15.7 | 23.6 |
| | CI | 26.1–105.4 | 26.2–2316 | 11.0–16.0 | 17.9–43.0 | VW | 36.6–180.8 | 11.6–16.6 | 21.4–36.9 | 47.7–57.9 | 47.9–87.7 | 13.9–17.6 | 21.8–25.5 |
| Nuclear Area | $EC_{20}$ | NS | NS | 20.8 | NS | NS | NS | 18.1 | NS | NS | 108.1 | 12.5 | 26.4 |
| | CI | | | VW | | | | VW | | | 54.3–215 | VW | VW |
| P2A | $EC_{20}$ | NS | NS | 8.7 | NS | NS | NS | 8.3 | NS | NS | — | 7.7 | 33.8 |
| | CI | | | 7.8–9.9 | | | | 7.4–9.2 | | | — | 6.5–9.1 | 25.8–44.3 |
| LWR | $EC_{20}$ | NS | NS | 6.8 | NS | NS | NS | 7.6 | NS | 70.9 | 61.8 | 6.1 | 11.8 |
| | CI | | | 3.5–13.0 | | | | 5.7–10.0 | | 32.5–154.3 | 35.3–108.2 | 5.3–7.1 | 5.7–24.4 |
| Cell Cycle (Sub G1) | $EC_{20}$ | NS | NS | 5.8 | NS | NS | NS | 6.3 | 13.7 | — | NS | 0.4 | 0.3 |
| | CI | | | 3.6–9.2 | | | | 2.9–13.5 | 4.7–40.0 | — | | 0.03–4.2 | 0.05–1.6 |
| Cell Cycle (G0/1) | $EC_{20}$ | NS | NS | 11.4 | — | NS | NS | 10.1 | 38.0 | NS | NS | 9.8 | 18.9 |
| | CI | | | 6.1–21.3 | — | | | VW | 20.6–70.0 | | | 9.4–10.2 | 15.8–22.5 |
| Cell Cycle (S) | $EC_{20}$ | NS | NS | 19.3 | 8.8 | NS | NS | 17.12 | 5.7 | NS | NS | 8.6 | 23.5 |
| | CI | | | VW | VW | | | VW | VW | | | 7.0–10.1 | 9.0–62.1 |
| Cell Cycle (G2/M) | $EC_{20}$ | 54.6 | NS | 11.9 | 25.2 | NS | — | 9.8 | 52.2 | NS | NS | 12.0 | 24.7 |
| | CI | VW | | VW | VW | | — | 9.2–10.5 | 13.8–198.1 | | | VW | 21.7–28.1 |
| BrdU | $EC_{20}$ | NS | 36.9 | 10.7 | NS | — | 78 | 10.4 | NS | NS | NS | 12.2 | NS |
| | CI | | 15.8–86.2 | 8.6–13.3 | | — | 12.9–472.4 | VW | | | | 18.3–81.8 | |
| γ-H2AX | $EC_{20}$ | NS | 31.0 | 10.9 | NS | 50.3 | 20.6 | 11.2 | NS | 60.2 | 56.6 | 11.3 | 26.1 |
| | CI | | 9.5–101.1 | 8.7–13.7 | | VW | 9.9–42.9 | VW | | VW | VW | VW | |
| F-actin | $EC_{20}$ | 7.5 | 4.5 | 7.8 | 10.1 | 31.5 | 66.2 | 10.2 | 24.4 | 47.0 | 99.4 | 10.9 | 24.6 |
| | CI | 1.7–34.0 | 0.7–28.6 | 5.5–11.1 | 5.8–20.5 | 12.4–80.0 | 36.2–121.1 | VW | 20.1–28.4 | 41.1–53.8 | 39.2–252.1 | VW | VW |

Notes. $EC_{20}$: Values for does causing 20% of the maximum response. CI: 95% confidence interval. NS: not significant. ND: not determined. VW: very wide; —, $EC_{20}$ simulation failed (exceeded treatment concentration that decreased cell viability to 0%). Color code: red, increase; green, decrease.

[a]Data from NR uptake assay.

perturbation (31.5 μM), followed by DNA damage responses (50.3 μM) and cell number decrease (50 μM). After 72 h treatment, the EC20 for multiple cellular responses was at the same dose level (50 μM). For the BPS treatment, the endpoint with the lowest EC20 was cytoskeleton perturbation (4.5 μM), followed by DNA damage responses (31.0 μM), DNA synthesis inhibition (36.9 μM) and cell number decrease (246.1 μM) after 24 h treatment. After 48 h treatment, the endpoint with the lowest EC20 was DNA damage responses (20.5 μM) followed by cytoskeleton perturbation (66.2 μM) and cell number decrease (81.4 μM). After 72 h treatment, BPS induced nuclear shape changes, cell cycle arrest, and DNA damage responses all at the same doses of 50 μM, while for cytoskeleton perturbation and nuclear area changes, the EC20 values were around 100 μM. BPAF treatment induced a wide spectrum of cellular events at a concentration of approximate 10 μM. These changes were independent of the time of exposure, and include decreases of cell numbers, changes of cell number, nuclear morphology, cell cycle perturbations, DNA synthesis facilitation, increased DNA damage responses and cytoskeleton perturbations. The induction of apoptotic cells showed the lowest EC20 values (0.4 μM) after 72 h treatment. Among these endpoints, LWR consistently showed lower EC20 values (6.1-7.6 μM), suggesting that alteration of nuclear roundness could serve as an early sensitive marker of BPAF toxicity in C-18 spermatogonial cells. For the TBBPA treatment, the endpoints with the lowest EC20 were S phase decrease (8.8 μM) followed by cytoskeleton perturbation (10.1 μM), G2/M phase increase, and cell number decrease around 25 μM after 24 h treatment. After 48 h treatment, the endpoint with the lowest EC20 was S phase decrease (5.7 μM) followed by apoptosis increase (13.7 μM), cytoskeleton perturbation (24.4 μM), cell number decrease (28.1 μM), G0/1 phase decrease (38 μM) and G2/M phase increase (52.2 μM). After 72 h treatment, TBBPA treatment induced various cellular responses at a concentration of approximately 25 μM (EC20), except for apoptosis increase. In summary, in comparison of the EC20 values of four bisphenols, BPAF stood out markedly, with high cytotoxicity (EC20 values ranging from 0.4 to 20 μM). TBBPA was identified as having an intermediate toxicity (EC20 values ranging from 0.3 to 47 μM). BPA and BPS were less cytotoxic (EC20 values from 4.5 to 250 μM) and the differences between these two compounds were minor.

In summary, we established the HCA/HTP assay in the 3D-SGC model and generated and modeled R/D toxicity for evaluating the bisphenol A and analogies compounds. Generation of dose and time dependent *in vitro* data in the 3D-TCCS model by using new HTP assays on signaling pathways such as cell cycle and DNA damage validated our 3D-TCCS for R/D toxicity screening. These HTP data can be linked with computational models to improve the understanding of the critical role of cell signaling pathways in R/D toxicity, make prediction of adverse effects from exposure, and pave the way for both accelerated testing of toxicants and significantly reduced use of animals. Pathway-based assays provide information on mode of action of compounds on R/D toxicity.

**Discussion:**

Despite increasing use of BPA analogues as BPA alternatives, there are still limited data available on their reproductive toxicities. Assessing reproductive toxins poses great challenges, therefore it is urgent to develop an improved *in vitro* model to identify and assess critical biological events leading to adverse reproductive outcomes. Cytotoxicity is a very complex process affecting multiple signaling pathways within cells. New approaches for toxicity characterization have focused on *in vitro* high-throughput and high-content assays, which enable measurement of early, sub-lethal indicators of cellular toxicity, as well as determination of the sequences and patterns of cellular events. HCA has been an effective and sensitive tool for obtaining large quantities of robust data on the multiple effects of compounds as compared

with conventional cytotoxicity assays like the NR assay. Several studies demonstrated that data obtained with HCA are concordant with drug-induced toxicity in humans [101, 103, 104]. HCA has been widely used to assess chemical-induced mechanistic effects, and has been applied to drug discovery using specific cell type or three-dimensional cell culture models [113-117]. In this study, we developed and validated a number of HCA-based assays and phenotypic read-outs, including characterizations of nuclear morphology, DNA content, cell cycle, cytoskeleton integrity, and DNA damage responses using a germline cell line.

Changes in nuclear morphology are general a reflection or a result of accumulation, of millions of cellular events taking place inside a cell, and known to be tightly associated with proliferation, gene expression, and protein synthesis [118]. The nucleus is surrounded by the nuclear envelope, which isolates chromosomes from cytoplasm and typically has either an oval or round shape. Previous studies have demonstrated that the changes in nuclear morphology seen with HCA were sensitive markers for detecting cytotoxic effects [101, 111, 119]. In the present study, we found that BPA induced alterations of nuclear shape (LWR) at non-cytotoxic doses, which is similar to previous findings in mouse embryonic fibroblasts [120, 121]. An *in vivo* study recently demonstrated that low-dose exposure to BPA (2μg/kg) induced germ cell apoptosis in adult rats [122]. Interestingly, we observed that BPAF induced a dose-dependent increase of multinucleated cells. Induction of abnormal testicular germ cells, such as multinucleated germ cells (MNGs), has been reported following gestational exposure to di-(n-butyl) phthalate (DBP) [123-126]. Ferrara and colleagues speculated that germ cells presenting DBP-induced MNGs may develop into carcinoma *in situ* (CIS) cells, the known precursors of testicular germ cell tumors (TGCT) in men [127]. Cell cycle analysis revealed that these BPAF-induced multinucleated cells were actively synthesizing DNA (BrdU), with increased numbers of cells in S and G2/M phase, suggesting these germline cells underwent abnormal proliferation. Further animal studies are need to confirm whether BPAF has a testicular toxicity similar to DBP *in vivo.*

Assessment of the cell cycle status of individual cells is pivotal for the evaluation of cell cycle regulation in response to intracellular and extracellular cues. Cell cycle status and progression has traditionally been measured using population-based methods such as flow cytometry [128, 129]. Flow cytometry is generally dependent on the successful preparation of a single-cell suspension, which is not compatible with high-throughput and high-resolution cell imaging. HCA-based cell cycle analysis was recently reported by Roukos et al [110]. Cell cycle profiles with discrete G1, S or G2/M populations were determined and these results were comparable to data obtained from flow cytometry analysis [110]. We have established a protocol for the spermatogonial cell line, which was able to accurately segment the nuclei for DNA content quantification. We have shown the dynamic changes of the cell cycle in the control population at different time-points (Table 1). Those percentage changes across the phases of the cell cycle are consistent with the cellular growth status, exhibiting fast proliferation at an early time-point and then slowing down when cells reach 100% confluence for 72 h. This HCA-based cell cycle analysis allows us to be able to accurately segment the nuclei even when the C18-4 spermatogonial cells were at 100% confluence for 72 h. As an imaging-based method to probe the cell cycle phase of individual cells, HCA can be used to correlate phases with the subcellular localization or the co-expression levels of multiple DNA loci or proteins tagged with different fluorescent markers. This feature will be widely applied in the mechanistic toxicity studies to screen or identify potential mechanisms of action. As revealed in the cell cycle analysis using HCA-based DNA content histograms and BrdU incorporation assay, we found that BPA and its analogues induced dose- and time-dependent alterations of the cell cycle with chemical specific changes Previous *in vivo* studies showed that BPA disrupted meiosis I progression and altered the number of leptotene and diplotene spermatocytes percentages in rat testicular cells [130, 131]. Disruption of the cell cycle has been proposed to be a key event in BPA testicular toxicity [130, 131]. Our results demonstrated that BPA or BPS treatments at a

concentration of 10 or 50 □M disrupted mitosis progression (G2/M phase). BPA induced dose-dependent decrease of BrdU positive cells for 48 h, suggesting that HCA-based quantification of BrdU is a sensitive endpoint for the evaluation of the cell cycle on comparison to the cell cycle profiling from total DNA content histogram. It has been reported that BPA exposure caused diverse effects on the cell cycle. BPA treatment can inhibit cell proliferation and induced S and G2/M phase arrest in midbrain cells at $1x10^{-4}$ M [130]. On the other side, low-dose BPA (≤$10^{-9}$ M) can promote cell proliferation in human seminoma cells though a G-protein-coupled non-classical membrane estrogen receptor (ER) and induced cell proliferation and cell-cycle regulatory proteins in human breast cell lines [132-134]. The differences between our current observations and previous studies may be due to the different sensitivity to the endpoints tested in spermatogonial cells. For BPAF treatment, along with the significant changes of nuclear morphology, we observed significant increases of S phase in both cell cycle profiling and BrdU labeling, and accumulation of cells in G2/M phase in a dose-dependent manner. Again, HCA-based assessment of the cell cycle status of individual cells suggested that BPAF treatment could result in significant alterations of cell cycle as compared to the treatment with BPA, BPS or TBBPA at similar dose ranges.

BPA has long been suspected to induce carcinogenesis [135]. Low doses of BPA have been reported to promote DNA damage, potentially contributing to breast cancer [133]. Several assays can measure and quantify cellular responses to DNA double-strand breaks. The proteins, such as γ–H2AX, ATM, CDKN1A, and TP53, involved in the early steps of the cellular response in sensing DNA damage and controlling progression, have been proposed as the top group of candidate biomarkers [136]. Due to the signal amplification of □H2AX foci at the site of DNA damage, the detection of γH2AX has been identified as an early sensitive cellular biomarker of DNA damage [137, 138]. In this study, we developed a multi-parametric HCA assay along with the detection of γH2AX and found that BPA and its analogues significantly altered the expression levels of γH2AX. It has been reported that BPA and its analogues induced DNA damages in a cell-type-specific and dose-dependent manner [139, 140]. BPA is able to induce DNA damage in spermatozoa (Liu, Duan et al. 2013), and in human breast cell line MCF-7 cells at the low concentration of 10 nM [130, 133]. Other studies showed that BPA at concentration of 100 μM did not induce γH2AX in a colorectal adenocarcinoma LSI174T cell line, but Bisphenol F did [141]. Most significantly, among all chemicals tested, BPAF showed significant induction of γH2AX at multiple time-points, suggesting a greater genotoxicity, as compared to other bisphenols.

The cytoskeleton, which serves as a scaffold that determines cell shape and the organization of the cytoplasm, plays a significant role in regulating cell shape, movement, cargo transportation and nuclear morphological modification [112]. Disorganization of F-actin was found to induce germ cells dysfunction *in vivo* [142]. A BPA exposure of 200 μM induced the truncation and de-polymerization of F-actin with mis-localization of actin regulatory proteins in human Sertoli cells without the changes of the total F-actin fluorescence intensity [143]. HCA-based analysis of F-actin demonstrated that all four bisphenols showed aberrant F-actin distribution in the cytoplasm (Figure 7B). These alterations in F-actin are highly correlated with the increased γH2AX expression, an early DNA damage responses marker (Table 3). It has been reported that alterations in the actin cytoskeleton were correlated with induction of γH2AX in human breast MCF-7 cells [144]. In the present study, comparison of EC20 values indicated F-actin appeared an early cellular response marker for chemical-induced testicular toxicity, and that perturbation of the cytoskeleton could potentially be associated with other endpoints, such as change of nuclear morphology and cell cycle alterations.

One of the applications of HCA assays in drug discovery and toxicity testing is prioritizing and ranking compounds for their potential human toxicity. By comparing of EC20

values among four bisphenols, BPAF showed the highest germ cell cytotoxicity, followed by TBBPA, BPA and BPS. Although the chemical structures of BPA and its analogues are similar, HCA demonstrated differential adverse effects of four bisphenols on multiple molecular and cellular events, suggesting that different mechanisms may promote cytotoxicity. Similar findings were reported in previous *in vitro* studies, in which BPAF and TBBPA showed higher endocrine modulating potentials in human MCF7 breast cancer cells and Leydig cells, respectively, as compared to BPA [145, 146]. BPS showed similar inhibitory effects with BPA on testosterone secretion in human fetal testes and induced more sensitive responses in mice testes [147]. By substituting different chemical groups and degree of halogenation, BPA and its analogues could exert differential toxicities via various receptor binding sites and binding affinities. In order to elucidate the potential structure-related toxicities, more BPA analogues will be included in future studies. Our *in vitro* data were also consistent with previous *in vivo* findings. BPA exposure (≤ 50mg/kg) consistently induced impairments of sperm production and quality, and alteration of steroidogenesis [148, 149]. Whereas BPS, BPAF and TBBPA exerted some adverse reproductive effects, including alterations of hormone levels, decreases in sperm count and changes of seminiferous epithelium morphology, Future study will be important to validate these findings [150-152].

In summary, we have developed multi-parametric HCA assays in germline cells and compared the testicular toxicity of BPA to some of its analogues. This multi-dimensional toxicological profiling revealed differential testicular toxicities of BPA and its analogues, whereas BPAF and TBBPA showed greater cytotoxicity, followed by BPA and BPS. Our findings also suggested that using the HCA platform with C18-4 spermatogonial cells could provide a rapid and cost-efficient tool to gain insights into mechanisms of toxicity, and establish links between molecular pathways and accelerate safety testing of potential reproductive toxicants.

## Publications

***Journal Article***


1. Liang, S., Yin, L., K. Yu, Hofmann,M & Yu, X. (2016). High-content Analysis Provides Mechanistic Insights into the Testicular Toxicity of Bisphenol A and Selected Analogues in Mouse Spermatogonial Cells. Toxicol. Sci. first published online September 14, 2016 doi:10.1093/toxsci/kfw178
2. Yin, L., Yu, K. S.,Simon Lin, Xiao Song, & Yu, X. (2016). Associations of blood mercury, inorganic mercury, methyl mercury and bisphenol A with dental surface restorations in the U.S. population, NHANES 2003-2004 and 2010-2012. Ecotoxicol Environ Saf. 2016 Dec;134P1:213-225. doi: 10.1016/j.ecoenv.2016.09.001
   Altmetric 740, Time Magazine, ADA, ScienceDaily, ScienceAlert, Dentistrytoday, UGA Today,
3. Yin, L., Yu, K. S., Lu, K., & Yu, X. (2016). Benzyl butyl phthalate promotes adipogenesis in 3T3-L1 preadipocytes: A High Content Cellomics and metabolomic analysis.. Toxicology in vitro, Jan 25;32:297-309. doi: 10.1016/j.tiv.2016.01.010
4. Harris, S., Hermsen, S. A. B., **Yu, X**., Hong, S. W., & Faustman, E. M. (2015). Comparison of toxicogenomic responses to phthalate ester exposure in an organotypic testis co-culture model and responses observed in vivo. REPRODUCTIVE TOXICOLOGY, 58, 149-159. doi:10.1016/j.reprotox.2015.10.002
5. Rawlance Ndejjo, Geofrey Musinguzi, Xiaozhong Yu, Esther Buregyeya, David Musoke, Jia-Sheng Wang, Abdullah Ali Halage, Christopher Whalen, William Bazeyo, Phillip Williams, John Ssempebwa, Occupational Health Hazards among Healthcare Workers in Kampala, Uganda. Journal of Environmental and Public Health 2015, ID 913741,

doi:10.1155/2015/913741

6. Garner, C.E., *S. Liang, L. Yin, and **X. Yu**, Physiologically based pharmacokinetic modeling for 1-bromopropane in F344 rats using gas uptake inhalation experiments. Toxicol Sci, 2015. First published online January 28, 2015 doi:10.1093/toxsci/kfv018
7. *Wegner, S.H., **X. Yu**, S. Pacheco Shubin, W.C. Griffith, and E.M. Faustman, Stage-specific signaling pathways during murine testis development and spermatogenesis: A pathway-based analysis to quantify developmental dynamics. Reprod Toxicol, 2014. 51C:31-39. doi:10.1016/j.reprotox.2014.11.008
8. Wegner, S.H., **X. Yu**, H. Kim, S. Harris, W.C. Griffith, S.H. Hong, and E.M. Faustman, Effect of dipentyl phthalate in 3-dimensional in vitro testis co-culture is attenuated by cyclooxygenase-2 inhibition. JTEHS, 2014. 6:161-169. doi:10.5897/JTEHS2014.0314
9. Garner, C.E. and **X. Yu**, Species and sex-dependent toxicokinetics of 1-bromopropane: the role of hepatic cytochrome P450 oxidation and glutathione (GSH). Xenobiotica, 2014. 44:644-56. doi:10.3109/00498254.2013.879624
10. Louise Parks Saldutti, Bruce Beyer, William Breslin, Terry R. Brown, Robert E. Chapin, Sarah Campion, Brian Enright, Elaine Faustman, Paul Foster, William Kelce, James H. Kim, Elizabeth G. Loboa, Aldert H. Piersma, David Seyler, Katie Turner, Hanry Yu, **Xiaozhong Yu**, Jennifer C. Sasaki, In vitro Testicular Toxicity Models: Opportunities for Advancement via Biomedical Engineering Techniques, ALTEX. 2013;30(3):353-77.
11. Wegner S, Hong S, **Yu X**, Faustman EM. Preparation of Rodent Testis Co-Cultures. Current Protocols in Toxicology 16.10.1-16.10.7, February 2013. doi:10.1002/0471140856.tx1610s55
12. McConnachie, L.A., D. Botta, C.C. White, C.S. Weldy, H.W. Wilkerson**, X. Yu** et al., *The glutathione synthesis gene Gclm modulates amphiphilic polymer-coated CdSe/ZnS quantum dot-induced lung inflammation in mice.* PLoS One, 2013. 8:e64165. doi:10.1371/journal.pone.0064165

**Manuscript under submission or preparation**

1. Yin, L., Hong Ye Wei., & Yu, X. (2016). An *in vitro* testicular cells co-culture model for evaluation male reproductive toxicants, Tox Sci, submitted
2. Yin, L.& Yu, X. (2016). Quantitative High-content analysis of cadmium induced alterations in cell cycle and phosphate H2AX DNA damage in spermatogonia cell, Reproductive Tox, submitted
3. Yin, L. Shenxuan Liang & Yu, X. (2016). Quantitative High-content analysis of NTP 80/91 chemical library in nuclear morphology, cell cycle and phosphate H2AX DNA damage in a three-dimentional testicular cell co-culture. In preparation
4. Shenxuan Liang, Yin, L. & Yu, X. (2016). Machine learning based high-content image analysis of NTP 80/91 chemical library in a three-dimentional testicular cell co-culture. In preparation
5. Yin, L. Shenxuan Liang & Yu, X. (2016). Quantitative High-content analysis of NTP 80/91 chemical library in the nuclear morphology, cell cycle and phosphate H2AX DNA damage in a three-dimentional testicular cell co-culture. In preparation
6. Yin, L. Shenxuan Liang & Yu, X. (2016). Quantitative High-content analysis of NTP 80/91 chemical library in the phagocytosis marker LC3B in comapration to nuclear morphology, cell cycle and phosphate H2AX DNA damage in a three-dimentional testicular cell co-culture. In preparation
7. Yin, L. Shenxuan Liang & Yu, X. (2016). Quantitative High-content analysis of NTP 80/91 chemical library in the epigenetic marker MBD-1 in comapration to nuclear morphology, cell cycle and phosphate H2AX DNA damage in a three-dimentional testicular cell co-culture. In preparation
8. Measel, E., Yin, L. Shenxuan Liang & Yu, X. (2016). Bisphenol AF (BPAF) induced mega-nucleus through the disruptions of nuclear envelop proteins Lamin A and LNC complex in

mouse spermatogonia cell. In preparation

***Proceedings***

1. Shenxuan Liang, L Yin and X Yu: An *in vitro* Testicular Cells Co-Culture Model for Assessing Testicular Toxicities of BPA and its Analogues Using High-content Analysis Southeastern SOT, Oct. 17, 2016
2. Shenxuan Liang, L Yin and X Yu: Cell-based High-content Analysis (HCA) Reveals Differential Effects of BPA and its Selected Analogues on Spermatogonia Stem Cells SOT Toxicologist, March 2016
3. Lei Yin, Tanzilal Mowla, X Yu: Epigenetic Regulation of Chlorpyrifos Induced Adipogenesis Using 3T3-L1 In Vitro Model, SOT Toxicologist March 2016.
4. Lei Yin, Tanzilal Mowla, X Yu: High Content Analysis (HCA) of Effects of Low-dose Cadmium on DNA Damage and Cell Cycle in Spermatogonial Stem Cells, SOT Toxicologist, March 2016
5. X Yu, Hongye Wei, Lei Yin: *In vitro* "mini-testis" model for male reproductive Toxicity: Opportunities for Advancement via Biomedical Engineering Techniques, the 7th National Congress of Toxicology, Chinese Society of Toxicology, Oct 25-30, Wuhan China
6. H Wei, L Yin and X Yu: *In Vitro* Spermatogenesis Model for Assessing Male Reproductive Toxicity SOT Toxicologist, March 2015; 144: p250.
7. S Liang, Garner E, LYin and X Yu: Physiologically Based Pharmacokinetic Modeling for 1-Bromoproane in Rat Using Gas Uptake Inhalation Studies SOT Toxicologist March 2015; 144: p161.
8. L Yin, S Yu, Hongye Wei, and X Yu. Environmental Exposure to Benzyl Butyl Phthalate Promotes Adipogenesis in the Preadipocyte 3T3-L1 SOT Toxicologist March 2015; 144: p365.
9. L Yin and X Yu. Bisphenol A (BPA) affects the spermatogenesis by disrupting gene regulations in glycomics. Society of Teratology Meeting 2014, Birth Defects Research (Part A) 100:319–357

**References**


1. National Research Council, *Toxicity Testing in the 21st Century: A Vision and a Strategy*. 2007, National Academies Press: Washington, DC.
2. Stillerman, K.P., D.R. Mattison, L.C. Giudice, and T.J. Woodruff, *Environmental exposures and adverse pregnancy outcomes: A review of the science.* Reproductive Sciences, 2008. **15**(7): p. 631-650.
3. Kim, Y., K. Jung, T. Hwang, G. Jung, H. Kim, J. Park, J. Kim, D. Park, S. Park, K. Choi, and Y. Moon, *Hematopoietic and reproductive hazards of Korean electronic workers exposed to solvents containing 2-bromopropane.* Scand J Work Environ Health, 1996. **22**(5): p. 387-91.
4. Yu, X., G. Ichihara, J. Kitoh, Z. Xie, E. Shibata, M. Kamijima, N. Asaeda, N. Hisanaga, and Y. Takeuchi, *Effect of inhalation exposure to 2-bromopropane on the nervous system in rats.* Toxicology, 1999. **135**(2-3): p. 87-93.
5. Yu, X., G. Ichihara, J. Kitoh, Z. Xie, E. Shibata, M. Kamijima, and Y. Takeuchi, *Neurotoxicity of 2-bromopropane and 1-bromopropane, alternative solvents for chlorofluorocarbons.* Environ Res, 2001. **85**(1): p. 48-52.
6. Yu, X., M. Kamijima, G. Ichihara, W. Li, J. Kitoh, Z. Xie, E. Shibata, N. Hisanaga, and Y. Takeuchi, *2-Bromopropane causes ovarian dysfunction by damaging primordial follicles and their oocytes in female rats.* Toxicol Appl Pharmacol, 1999. **159**(3): p. 185-93.
7. Yu, X., H. Kubota, R. Wang, J. Saegusa, Y. Ogawa, G. Ichihara, Y. Takeuchi, and N. Hisanaga, *Involvement of Bcl-2 family genes and Fas signaling system in primary and secondary male germ cell apoptosis induced by 2-bromopropane in rat.* Toxicol Appl Pharmacol, 2001. **174**(1): p. 35-48.
8. Yu, X.Z., G. Ichihara, J. Kitoh, Z.L. Xie, E. Shibata, M. Kamijima, N. Asaeda, N. Hisanaga, and Y. Takeuchi, *Effect of inhalation exposure to 2-bromopropane on the nervous system in rats.* Toxicology,

1999. **135**(2-3): p. 87-93.
9. Yu, X.Z., G. Ichihara, J. Kitoh, Z.L. Xie, E. Shibata, M. Kamijima, N. Asaeda, and Y. Takeuchi, *Preliminary report on the neurotoxicity of 1-bromopropane, an alternative solvent for chlorofluorocarbons.* J Occup Health, 1998. **40**(3): p. 234-235.
10. Yu, X.Z., G. Ichihara, J. Kitoh, Z.L. Xie, E. Shibata, M. Kamijima, and Y. Takeuchi, *Neurotoxicity of 2-bromopropane and 1-bromopropane, alternative solvents for chlorofluorocarbons.* Environ Res, 2001. **85**(1): p. 48-52.
11. Yu, X.Z., M. Kamijima, G. Ichihara, W.X. Li, J. Kitoh, Z.L. Xie, E. Shibata, N. Hisanaga, and Y. Takeuchi, *2-bromopropane causes ovarian dysfunction by damaging primordial follicles and their oocytes in female rats.* Toxicol Appl Pharmacol, 1999. **159**(3): p. 185-193.
12. Yu, X.Z., H. Kubota, R.S. Wang, J. Saegusa, Y. Ogawa, G. Ichihara, Y. Takeuchi, and N. Hisanaga, *Involvement of Bcl-2 family genes and Fas signaling system in primary and secondary male germ cell apoptosis induced by 2-bromopropane in rat.* Toxicol Appl Pharmacol, 2001. **174**(1): p. 35-48.
13. Ichihara, G., X. Ding, X. Yu, X. Wu, M. Kamijima, S. Peng, X. Jiang, and Y. Takeuchi, *Occupational health survey on workers exposed to 2-bromopropane at low concentrations.* Am J Ind Med, 1999. **35**(5): p. 523-31.
14. Ichihara, G., X.C. Ding, X.Z. Yu, X.D. Wu, M. Kamijima, S.M. Peng, X.Z. Jiang, and Y. Takeuchi, *Occupational health survey on workers exposed to 2-bromopropane at low concentrations.* Am J Ind Med, 1999. **35**(5): p. 523-531.
15. Ichihara, G., J. Kitoh, X. Yu, N. Asaeda, H. Iwai, T. Kumazawa, E. Shibata, T. Yamada, H. Wang, Z. Xie, and Y. Takeuchi, *1-Bromopropane, an alternative to ozone layer depleting solvents, is dose-dependently neurotoxic to rats in long-term inhalation exposure.* Toxicol Sci, 2000. **55**(1): p. 116-23.
16. Ichihara, G., J. Kitoh, X.Z. Yu, N. Asaeda, H. Iwai, T. Kumazawa, E. Shibata, T. Yamada, H.L. Wang, Z.L. Xie, and Y. Takeuchi, *1-bromopropane, an alternative to ozone layer depleting solvents, is dose-dependently neurotoxic to rats in long-term inhalation exposure.* Toxicological Sciences, 2000. **55**(1): p. 116-123.
17. Ichihara, G., W. Li, X. Ding, S. Peng, X. Yu, E. Shibata, T. Yamada, H. Wang, S. Itohara, S. Kanno, K. Sakai, H. Ito, K. Kanefusa, and Y. Takeuchi, *A survey on exposure level, health status, and biomarkers in workers exposed to 1-bromopropane.* Am J Ind Med, 2004. **45**(1): p. 63-75.
18. Ichihara, G., W.H. Li, X.C. Ding, S.M. Peng, X.Z. Yu, E. Shibata, T. Yamada, H.L. Wang, S. Itohara, S. Kanno, K. Sakai, H. Ito, K. Kanefusa, and Y. Takeuchi, *A survey on exposure level, health status, and biomarkers in workers exposed to 1-bromopropane.* Am J Ind Med, 2004. **45**(1): p. 63-75.
19. Ichihara, G., X. Yu, J. Kitoh, N. Asaeda, T. Kumazawa, H. Iwai, E. Shibata, T. Yamada, H. Wang, Z. Xie, K. Maeda, H. Tsukamura, and Y. Takeuchi, *Reproductive toxicity of 1-bromopropane, a newly introduced alternative to ozone layer depleting solvents, in male rats.* Toxicol Sci, 2000. **54**(2): p. 416-23.
20. Ichihara, G., X.Z. Yu, J. Kitoh, N. Asaeda, T. Kumazawa, H. Iwai, E. Shibata, T. Yamada, H.L. Wang, Z.L. Xie, K. Maeda, H. Tsukamura, and Y. Takeuchi, *Reproductive toxicity of 1-bromoprapane, a newly introduced alternative to ozone layer depleting solvents, in male rats.* Toxicological Sciences, 2000. **54**(2): p. 416-423.
21. Ichihara, G., N. Asaeda, T. Kumazawa, Y. Tagawa, M. Kamijima, X.Z. Yu, H. Kondo, T. Nakajima, J. Kitoh, I.J. Yu, Y.H. Moon, N. Hisanaga, and Y. Takeuchi, *Testicular and hematopoietic toxicity of 2-bromopropane, a substitute for ozone layer-depleting chlorofluorocarbons.* J Occup Health, 1997. **39**(1): p. 57-63.
22. Wang, H., G. Ichihara, H. Ito, K. Kato, J. Kitoh, T. Yamada, X. Yu, S. Tsuboi, Y. Moriyama, R. Sakatani, E. Shibata, M. Kamijima, S. Itohara, and Y. Takeuchi, *Biochemical changes in the central nervous system of rats exposed to 1-bromopropane for seven days.* Toxicol Sci, 2002. **67**(1): p. 114-20.
23. Wang, H.L., G. Ichihara, H. Ito, K. Kato, J. Kitoh, T. Yamada, X.Z. Yu, S. Tsuboi, Y. Moriyama, and Y. Takeuchi, *Dose-dependent biochemical changes in rat central nervous system after 12-week exposure to 1-bromopropane.* Neurotoxicology, 2003. **24**(2): p. 199-206.
24. Blystone, C.R., G.E. Kissling, J.B. Bishop, R.E. Chapin, G.W. Wolfe, and P.M. Foster, *Determination of the di-(2-ethylhexyl) phthalate NOAEL for reproductive development in the rat: importance of the retention of extra animals to adulthood.* Toxicol Sci, 2010. **116**(2): p. 640-6.
25. Hotchkiss, A.K., C.V. Rider, C.R. Blystone, V.S. Wilson, P.C. Hartig, G.T. Ankley, P.M. Foster, C.L. Gray,

and L.E. Gray, *Fifteen years after "Wingspread"--environmental endocrine disrupters and human and wildlife health: where we are today and where we need to go.* Toxicol Sci, 2008. **105**(2): p. 235-59.

26. Knudsen, T.B., K.A. Houck, N.S. Sipes, A.V. Singh, R.S. Judson, M.T. Martin, A. Weissman, N.C. Kleinstreuer, H.M. Mortensen, D.M. Reif, J.R. Rabinowitz, R.W. Setzer, A.M. Richard, D.J. Dix, and R.J. Kavlock, *Activity profiles of 309 ToxCast chemicals evaluated across 292 biochemical targets.* Toxicology, 2010. **282**(1-2): p. 1-15.
27. Reif, D.M., M.T. Martin, S.W. Tan, K.A. Houck, R.S. Judson, A.M. Richard, T.B. Knudsen, D.J. Dix, and R.J. Kavlock, *Endocrine profiling and prioritization of environmental chemicals using ToxCast data.* Environ Health Perspect, 2010. **118**(12): p. 1714-20.
28. Genschow, E., H. Spielmann, G. Scholz, A. Seiler, N. Brown, A. Piersma, M. Brady, N. Clemann, H. Huuskonen, F. Paillard, S. Bremer, and K. Becker, *The ECVAM international validation study on in vitro embryotoxicity tests: results of the definitive phase and evaluation of prediction models. European Centre for the Validation of Alternative Methods.* Altern Lab Anim, 2002. **30**(2): p. 151-76.
29. Piersma, A.H., E. Genschow, A. Verhoef, M.Q. Spanjersberg, N.A. Brown, M. Brady, A. Burns, N. Clemann, A. Seiler, and H. Spielmann, *Validation of the postimplantation rat whole-embryo culture test in the international ECVAM validation study on three in vitro embryotoxicity tests.* Altern Lab Anim, 2004. **32**(3): p. 275-307.
30. Spielmann, H., E. Genschow, N.A. Brown, A.H. Piersma, A. Verhoef, M.Q. Spanjersberg, H. Huuskonen, F. Paillard, and A. Seiler, *Validation of the rat limb bud micromass test in the international ECVAM validation study on three in vitro embryotoxicity tests.* Altern Lab Anim, 2004. **32**(3): p. 245-74.
31. Genschow, E., H. Spielmann, G. Scholz, I. Pohl, A. Seiler, N. Clemann, S. Bremer, and K. Becker, *Validation of the embryonic stem cell test in the international ECVAM validation study on three in vitro embryotoxicity tests.* Altern Lab Anim, 2004. **32**(3): p. 209-44.
32. Yu, X., J.S. Sidhu, S. Hong, and E.M. Faustman, *Essential role of extracellular matrix (ECM) overlay in establishing the functional integrity of primary neonatal rat Sertoli cell/gonocyte co-cultures: an improved in vitro model for assessment of male reproductive toxicity.* Toxicol Sci, 2005. **84**(2): p. 378-93.
33. Yu, X., E.M. Faustman, S. Hong, and J.S. Sidhu, *Effects of methyl mercury and cadmium on stress signaling and ubiquitination pathways in a primary Sertoli cell-gonocyte co-culture system.* Toxicological Sciences, 2003. **72**(1): p. 274-274.
34. Faustman, E.M., X.Z. Yu, and S.W. Hong, *Improving in vitro models for assessing male reproductive toxicity: Incorporating genomic considerations.* International Congress o f Toxicology Symposium on In vitro Toxicology – Evolving Concepts in Tissue Modeling, 2007. **June 15-19, Montreal,Canada**.
35. Yu, X.Z., S.W. Hong, and E.M. Faustman, *Germ-line stem cells-gonocytes as an /in vitro/ model for male developmental toxicity: comparison from cytotoxicity to genomic responses to phthalates.* Socitey of Toxicology, March 25-29, 2008. **Seattle, WA**.
36. Yu, X.Z., S.W. Hong, E. Kim, and E.M. Faustman, *In vitro 3-D Sertoli cell/gonocyte co-culture model in screening male reproductive toxicants* 6th World Congress on Alternatives & Animal Use in the Life Sciences, 2007. **August 21-26, Tokyo**.
37. Yu, X.Z., S.W. Hong, E. Kim, and E.M. Faustman, *Characterization of male reproductive toxicants in an in vitro 3-D Sertoli cell/gonocyte co-cultures.* Socitey of Toxicology, March 25-29, 2007. **Charlotte, NC**.
38. Gray, T.J., *Testicular toxicity in vitro: Sertoli-germ cell co-cultures as a model system.* Food Chem Toxicol, 1986. **24**(6-7): p. 601-5.
39. Hadley, M.A., S.W. Byers, C.A. Suarez-Quian, H.K. Kleinman, and M. Dym, *Extracellular matrix regulates Sertoli cell differentiation, testicular cord formation, and germ cell development in vitro.* J Cell Biol, 1985. **101**(4): p. 1511-22.
40. Chapin, R.E., T.J. Gray, J.L. Phelps, and S.L. Dutton, *The effects of mono-(2-ethylhexyl)-phthalate on rat Sertoli cell-enriched primary cultures.* Toxicol Appl Pharmacol, 1988. **92**(3): p. 467-79.
41. Lejeune, H., P. Sanchez, and J.M. Saez, *Enhancement of long-term testosterone secretion and steroidogenic enzyme expression in human Leydig cells by co-culture with human Sertoli cell-enriched preparations.* Int J Androl, 1998. **21**(3): p. 129-40.

*42.* Yang, J.M., M. Arnush, Q.Y. Chen,X.D. Wu, B. Pang, and X.Z. Jiang, *Cadmium-induced damage to*

*primary cultures of rat Leydig cells.* Reprod Toxicol, 2003. **17**(5): p. 553-60.
43. Bilinska, B., *Interaction between Leydig and Sertoli cells in vitro.* Cytobios, 1989. **60**(241): p. 115-26.
44. Griswold, M.D., *The central role of Sertoli cells in spermatogenesis.* Semin Cell Dev Biol, 1998. **9**(4): p. 411-6.
45. Mather, J.P., K.M. Attie, T.K. Woodruff, G.C. Rice, and D.M. Phillips, *Activin stimulates spermatogonial proliferation in germ-Sertoli cell cocultures from immature rat testis.* Endocrinology, 1990. **127**(6): p. 3206-14.
46. Orth, J.M. and W.F. Jester, Jr., *NCAM mediates adhesion between gonocytes and Sertoli cells in cocultures from testes of neonatal rats.* J Androl, 1995. **16**(5): p. 389-99.
47. Braydich-Stolle, L.K., B. Lucas, A. Schrand, R.C. Murdock, T. Lee, J.J. Schlager, S.M. Hussain, and M.C. Hofmann, *Silver nanoparticles disrupt GDNF/Fyn kinase signaling in spermatogonial stem cells.* Toxicol Sci, 2010. **116**(2): p. 577-89.
48. Braydich-Stolle, L., S. Hussain, J.J. Schlager, and M.C. Hofmann, *In vitro cytotoxicity of nanoparticles in mammalian germline stem cells.* Toxicol Sci, 2005. **88**(2): p. 412-9.
49. Gregotti, C., A. Di Nucci, L.G. Costa, L. Manzo, R. Scelsi, F. Berte, and E.M. Faustman, *Effects of thallium on primary cultures of testicular cells.* J Toxicol Environ Health, 1992. **36**(1): p. 59-69.
50. Li, L.H., W.F. Jester, Jr., and J.M. Orth, *Effects of relatively low levels of mono-(2-ethylhexyl) phthalate on cocultured Sertoli cells and gonocytes from neonatal rats.* Toxicol Appl Pharmacol, 1998. **153**(2): p. 258-65.
51. Orth, J.M., W.F. Jester, L.H. Li, and A.L. Laslett, *Gonocyte-Sertoli cell interactions during development of the neonatal rodent testis.* Curr Top Dev Biol, 2000. **50**: p. 103-24.
52. Harris, S., S.A. Hermsen, X. Yu, S.W. Hong, and E.M. Faustman, *Comparison of toxicogenomic responses to phthalate ester exposure in an organotypic testis co-culture model and responses observed in vivo.* Reprod Toxicol, 2015. **58**: p. 149-159.
53. Wegner, S.H., X. Yu, H. Kim, S. Harris, W.C. Griffith, S.H. Hong, and E.M. Faustman, *Effect of dipentyl phthalate in 3-dimensional in vitro testis co-culture is attenuated by cyclooxygenase-2 inhibition.* JTEHS, 2014. **6**(8): p. 161-169.
54. Wegner, S., S. Hong, X. Yu, and E.M. Faustman, *Preparation of rodent testis co-cultures.* Curr Protoc Toxicol, 2013. **Chapter 16**: p. Unit 16 10.
55. Yu, X., S. Hong, E.G. Moreira, and E.M. Faustman, *Improving in vitro Sertoli cell/gonocyte co-culture model for assessing male reproductive toxicity: Lessons learned from comparisons of cytotoxicity versus genomic responses to phthalates.* Toxicol Appl Pharmacol, 2009. **239**(3): p. 325-36.
56. Hofmann, M.C., L. Braydich-Stolle, L. Dettin, E. Johnson, and M. Dym, *Immortalization of mouse germ line stem cells.* Stem Cells, 2005. **23**(2): p. 200-10.
57. Hofmann, M.C., L. Braydich-Stolle, and M. Dym, *Isolation of male germ-line stem cells; influence of GDNF.* Developmental Biology, 2005. **279**(1): p. 114-124.
58. Brown, N.A., *Selection of test chemicals for the ECVAM international validation study on in vitro embryotoxicity tests. European Centre for the Validation of Alternative Methods.* Altern Lab Anim, 2002. **30**(2): p. 177-98.
59. Moorman, W.J., H.W. Ahlers, R.E. Chapin, G.P. Daston, P.M. Foster, R.J. Kavlock, J.S. Morawetz, T.M. Schnorr, and S.M. Schrader, *Prioritization of NTP reproductive toxicants for field studies.* Reprod Toxicol, 2000. **14**(4): p. 293-301.
*60.* CIRM, *Stem Cells in Predictive Toxicology* in *CIRM Workshop Report*

C.I.f.R. Medicine, Editor. 2008, California Institute for Regenerative Medicine: California.
61. Chapin, R.E. and D.B. Stedman, *Endless possibilities: stem cells and the vision for toxicology testing in the 21st century.* Toxicol Sci, 2009. **112**(1): p. 17-22.
62. Sidhu, J.S., R.A. Ponce, M.A. Vredevoogd, X. Yu, E. Gribble, S.W. Hong, E. Schneider, and E.M. Faustman, *Cell cycle inhibition by sodium arsenite in primary embryonic rat midbrain neuroepithelial cells.* Toxicol Sci, 2006. **89**(2): p. 475-84.
63. Repetto, G., A. del Peso, and J.L. Zurita, *Neutral red uptake assay for the estimation of cell viability/cytotoxicity.* Nature Protocols, 2008. **3**(7): p. 1125-1131.
*64.* Yu, X.Z., S. Hong, E.G. Moreira, and E.M. Faustman, *Improving in vitro Sertoli cell/gonocyte co-culture*

*model for assessing male reproductive toxicity: Lessons learned from comparisons of cytotoxicity versus genomic responses to phthalates.* Toxicology and Applied Pharmacology, 2009. **239**(3): p. 325-336.

65. Martin, M.T., T.B. Knudsen, D.M. Reif, K.A. Houck, R.S. Judson, R.J. Kavlock, and D.J. Dix, *Predictive model of rat reproductive toxicity from ToxCast high throughput screening.* Biol Reprod, 2011. **85**(2): p. 327-39.
66. Kligerman, A.D., R.R. Young, L.F. Stankowski, Jr., K. Pant, T. Lawlor, M.J. Aardema, and K.A. Houck, *An evaluation of 25 selected ToxCast chemicals in medium-throughput assays to detect genotoxicity.* Environ Mol Mutagen, 2014.
67. Sofikitis, N., E. Pappas, A. Kawatani, D. Baltogiannis, D. Loutradis, N. Kanakas, D. Giannakis, F. Dimitriadis, K. Tsoukanelis, I. Georgiou, G. Makrydimas, Y. Mio, V. Tarlatzis, M. Melekos, and I. Miyagawa, *Efforts to create an artificial testis: culture systems of male germ cells under biochemical conditions resembling the seminiferous tubular biochemical environment.* Hum Reprod Update, 2005. **11**(3): p. 229-59.
68. Steinberger, A. and E. Steinberger, *Differentiation of Rat Seminiferous Epithelium in Organ Culture.* J Reprod Fertil, 1965. **9**: p. 243-8.
69. Orth, J.M., M.P. McGuinness, J. Qiu, W.F. Jester, Jr., and L.H. Li, *Use of in vitro systems to study male germ cell development in neonatal rats.* Theriogenology, 1998. **49**(2): p. 431-9.
70. Hakovirta, H., A. Keiski, J. Toppari, M. Halmekyto, L. Alhonen, J. Janne, and M. Parvinen, *Polyamines and regulation of spermatogenesis: selective stimulation of late spermatogonia in transgenic mice overexpressing the human ornithine decarboxylase gene.* Mol Endocrinol, 1993. **7**(11): p. 1430-6.
71. Ceridono, M., P. Tellner, D. Bauer, J. Barroso, N. Alépée, R. Corvi, A. De Smedt, M.D. Fellows, N.K. Gibbs, E. Heisler, A. Jacobs, D. Jirova, D. Jones, H. Kandárová, P. Kasper, J.K. Akunda, C. Krul, D. Learn, M. Liebsch, A.M. Lynch, W. Muster, K. Nakamura, J.F. Nash, U. Pfannenbecker, G. Phillips, C. Robles, V. Rogiers, F. Van De Water, U.W. Liminga, H.-W. Vohr, O. Wattrelos, J. Woods, V. Zuang, J. Kreysa, and P. Wilcox, *The 3T3 neutral red uptake phototoxicity test: Practical experience and implications for phototoxicity testing – The report of an ECVAM–EFPIA workshop.* Regulatory Toxicology and Pharmacology, 2012. **63**(3): p. 480-488.
72. Zapor, L., *Toxicity of some phenolic derivatives--in vitro studies.* Int J Occup Saf Ergon, 2004. **10**(4): p. 319-31.
73. Seiler, A.E. and H. Spielmann, *The validated embryonic stem cell test to predict embryotoxicity in vitro.* Nat Protoc, 2011. **6**(7): p. 961-78.
74. Gray, L.E., Jr., J. Ostby, J. Furr, M. Price, D.N. Veeramachaneni, and L. Parks, *Perinatal exposure to the phthalates DEHP, BBP, and DINP, but not DEP, DMP, or DOTP, alters sexual differentiation of the male rat.* Toxicol Sci, 2000. **58**(2): p. 350-65.
75. Kumar, N., S. Srivastava, and P. Roy, *Impact of low molecular weight phthalates in inducing reproductive malfunctions in male mice: Special emphasis on Sertoli cell functions.* General and Comparative Endocrinology, 2015. **215**(0): p. 36-50.
76. Sung, H.H., W.Y. Kao, and Y.J. Su, *Effects and toxicity of phthalate esters to hemocytes of giant freshwater prawn, Macrobrachium rosenbergii.* Aquat Toxicol, 2003. **64**(1): p. 25-37.
77. Helmestam, M., E. Davey, A. Stavreus-Evers, and M. Olovsson, *Bisphenol A affects human endometrial endothelial cell angiogenic activity in vitro.* Reprod Toxicol, 2014. **46**: p. 69-76.
78. Chapin, R.E., J.L. Phelps, L.T. Burka, M.B. Abou-Donia, and J.J. Heindel, *The effects of tri-o-cresyl phosphate and metabolites on rat Sertoli cell function in primary culture.* Toxicol Appl Pharmacol, 1991. **108**(2): p. 194-204.
79. McKim, J.M., Jr., *Building a tiered approach to in vitro predictive toxicity screening: a focus on assays with in vivo relevance.* Comb Chem High Throughput Screen, 2010. **13**(2): p. 188-206.
80. Bouhifd, M., G. Bories, J. Casado, S. Coecke, H. Norlen, N. Parissis, R.M. Rodrigues, and M.P. Whelan, *Automation of an in vitro cytotoxicity assay used to estimate starting doses in acute oral systemic toxicity tests.* Food Chem Toxicol, 2012. **50**(6): p. 2084-96.
81. Chandler, K.J., M. Barrier, S. Jeffay, H.P. Nichols, N.C. Kleinstreuer, A.V. Singh, D.M. Reif, N.S. Sipes, R.S. Judson, D.J. Dix, R. Kavlock, E.S. Hunter, 3rd, and T.B. Knudsen, *Evaluation of 309 environmental chemicals using a mouse embryonic stem cell adherent cell differentiation and cytotoxicity assay.* PLoS

One, 2011. **6**(6): p. e18540.
82. Hareng, L., C. Pellizzer, S. Bremer, M. Schwarz, and T. Hartung, *The integrated project ReProTect: a novel approach in reproductive toxicity hazard assessment.* Reprod Toxicol, 2005. **20**(3): p. 441-52.
83. Balls, M. and J.H. Fentem, *The validation and acceptance of alternatives to animal testing.* Toxicol In Vitro, 1999. **13**(4-5): p. 837-46.
84. Foster, P.M., D.M. Creasy, J.R. Foster, L.V. Thomas, M.W. Cook, and S.D. Gangolli, *Testicular toxicity of ethylene glycol monomethyl and monoethyl ethers in the rat.* Toxicol Appl Pharmacol, 1983. **69**(3): p. 385-99.
85. Foster, P.M., D.M. Creasy, J.R. Foster, and T.J. Gray, *Testicular toxicity produced by ethylene glycol monomethyl and monoethyl ethers in the rat.* Environ Health Perspect, 1984. **57**: p. 207-17.
86. Starek-Swiechowicz, B., W. Szymczak, B. Budziszewska, and A. Starek, *Testicular effect of a mixture of 2-methoxyethanol and 2-ethoxyethanol in rats.* Pharmacol Rep, 2015. **67**(2): p. 289-93.
87. van der Laan, J.W., R.E. Chapin, B. Haenen, A.C. Jacobs, and A. Piersma, *Testing strategies for embryo-fetal toxicity of human pharmaceuticals. Animal models vs. in vitro approaches: a workshop report.* Regul Toxicol Pharmacol, 2012. **63**(1): p. 115-23.
88. Takei, M., Y. Ando, W. Saitoh, T. Tanimoto, N. Kiyosawa, S. Manabe, A. Sanbuissho, O. Okazaki, H. Iwabuchi, T. Yamoto, K.P. Adam, J.E. Weiel, J.A. Ryals, M.V. Milburn, and L. Guo, *Ethylene glycol monomethyl ether-induced toxicity is mediated through the inhibition of flavoprotein dehydrogenase enzyme family.* Toxicol Sci, 2010. **118**(2): p. 643-52.
89. Bagchi, G. and D.J. Waxman, *Toxicity of ethylene glycol monomethyl ether: impact on testicular gene expression.* Int J Androl, 2008. **31**(2): p. 269-74.
*90.* Bagchi, G., C.H. Hurst, and D.J. Waxman, *Interactions of methoxyacetic acid with androgen receptor.* Toxicol Appl Pharmacol, 2009. **238**(2): p. 101-10.
91. Foote, R.H., *Cadmium affects testes and semen of rabbits exposed before and after puberty.* Reprod Toxicol, 1999. **13**(4): p. 269-77.
92. Higuchi, T.T., J.S. Palmer, L.E. Gray, Jr., and D.N. Veeramachaneni, *Effects of dibutyl phthalate in male rabbits following in utero, adolescent, or postpubertal exposure.* Toxicol Sci, 2003. **72**(2): p. 301-13.
93. Veeramachaneni, D.N., J.S. Palmer, R.P. Amann, C.M. Kane, T.T. Higuchi, and K.Y. Pau, *Disruption of sexual function, FSH secretion, and spermiogenesis in rabbits following developmental exposure to vinclozolin, a fungicide.* Reproduction, 2006. **131**(4): p. 805-16.
94. Chapin, R.E., K. Boekelheide, R. Cortvrindt, M.B.M. van Duursen, T. Gant, B. Jegou, E. Marczylo, A.M.M. van Pelt, J.N. Post, M.J.E. Roelofs, S. Schlatt, K.J. Teerds, J. Toppari, and A.H. Piersma, *Assuring safety without animal testing: The case for the human testis in vitro.* Reproductive Toxicology, 2013. **39**: p. 63-68.
95. Olson, H., G. Betton, D. Robinson, K. Thomas, A. Monro, G. Kolaja, P. Lilly, J. Sanders, G. Sipes, W. Bracken, M. Dorato, K. Van Deun, P. Smith, B. Berger, and A. Heller, *Concordance of the toxicity of pharmaceuticals in humans and in animals.* Regul Toxicol Pharmacol, 2000. **32**(1): p. 56-67.
96. Ceridono, M., P. Tellner, D. Bauer, J. Barroso, N. Alepee, R. Corvi, A. De Smedt, M.D. Fellows, N.K. Gibbs, E. Heisler, A. Jacobs, D. Jirova, D. Jones, H. Kandarova, P. Kasper, J.K. Akunda, C. Krul, D.Learn, M. Liebsch, A.M. Lynch, W. Muster, K. Nakamura, J.F. Nash, U. Pfannenbecker, G. Phillips, C. Robles, V. Rogiers, F. Van De Water, U.W. Liminga, H.W. Vohr, O. Wattrelos, J. Woods, V. Zuang, J. Kreysa, and P. Wilcox, *The 3T3 neutral red uptake phototoxicity test: practical experience and implications for phototoxicity testing--the report of an ECVAM-EFPIA workshop.* Regul Toxicol Pharmacol, 2012. **63**(3): p. 480-8.
97. Kavlock, R., K. Chandler, K. Houck, S. Hunter, R. Judson, N. Kleinstreuer, T. Knudsen, M. Martin, S. Padilla, D. Reif, A. Richard, D. Rotroff, N. Sipes, and D. Dix, *Update on EPA's ToxCast Program: Providing High Throughput Decision Support Tools for Chemical Risk Management.* Chemical Research in Toxicology, 2012. **25**(7): p. 1287-1302.
98. Auerbach, S., D. Filer, D. Reif, V. Walker, A.C. Holloway, J. Schlezinger, S. Srinivasan, D. Svoboda, R. Judson, J.R. Bucher, and K.A. Thayer, *Prioritizing Environmental Chemicals for Obesity and Diabetes Outcomes Research: A Screening Approach Using ToxCast High Throughput Data.* Environ Health Perspect, 2016.
*99.* Karmaus, A.L., D.L. Filer, M.T. Martin, and K.A. Houck, *Evaluation of food-relevant chemicals in the*

*ToxCast high-throughput screening program.* Food and Chemical Toxicology, 2016. **92**: p. 188-96.
100. Paul Friedman, K., E.D. Watt, M.W. Hornung, J.M. Hedge, R.S. Judson, K.M. Crofton, K.A. Houck, and S.O. Simmons, *Tiered High-Throughput Screening Approach to Identify Thyroperoxidase Inhibitors Within the ToxCast Phase I and II Chemical Libraries.* Toxicological Sciences, 2016. **151**(1): p. 160-80.
101. O'Brien, P.J., W. Irwin, D. Diaz, E. Howard-Cofield, C.M. Krejsa, M.R. Slaughter, B. Gao, N. Kaludercic, A. Angeline, P. Bernardi, P. Brain, and C. Hougham, *High concordance of drug-induced human hepatotoxicity with in vitro cytotoxicity measured in a novel cell-based model using high content screening.* Archives of Toxicology, 2006. **80**(9): p. 580-604.
102. Xu, J.J., D. Diaz, and P.J. O'Brien, *Applications of cytotoxicity assays and pre-lethal mechanistic assays for assessment of human hepatotoxicity potential.* Chemico-Biological Interactions, 2004. **150**(1): p. 115-128.
103. Xu, J.J., P.V. Henstock, M.C. Dunn, A.R. Smith, J.R. Chabot, and D. de Graaf, *Cellular imaging predictions of clinical drug-induced liver injury.* Toxicological Sciences, 2008. **105**(1): p. 97-105.
104. Schoonen, W.G.E.J., J.A.D.M. de Roos, W.M.A. Westerink, and E. Debiton, *Cytotoxic effects of 110 reference compounds on HepG2 cells and for 60 compounds on HeLa, ECC-1 and CHO cells. II - Mechanistic assays on NAD(P)H, ATP and DNA contents.* Toxicology in Vitro, 2005. **19**(4): p. 491-503.
105. Ankley, G.T., R.S. Bennett, R.J. Erickson, D.J. Hoff, M.W. Hornung, R.D. Johnson, D.R. Mount, J.W. Nichols, C.L. Russom, P.K. Schmieder, J.A. Serrrano, J.E. Tietge, and D.L. Villeneuve, *Adverse Outcome Pathways: A Conceptual Framework to Support Ecotoxicology Research and Risk Assessment.* Environmental Toxicology and Chemistry, 2010. **29**(3): p. 730-741.
106. Perkins, E.J., P. Antczak, L. Burgoon, F. Falciani, N. Garcia-Reyero, S. Gutsell, G. Hodges, A. Kienzler, D. Knapen, M. McBride, and C. Willett, *Adverse Outcome Pathways for Regulatory Applications: Examination of Four Case Studies With Different Degrees of Completeness and Scientific Confidence.* Toxicological Sciences, 2015. **148**(1): p. 14-25.
107. Zhivotosky, B. and S. Orrenius, *Assessment of apoptosis and necrosis by DNA fragmentation and morphological criteria.* Current Protocols in Cell Biology, 2001. **Chapter 18**: p. Unit 18 3.
108. Elmore, S., *Apoptosis: A review of programmed cell death.* Toxicologic Pathology, 2007. **35**(4): p. 495-516.
109. Webster, M., K.L. Witkin, and O. Cohen-Fix, *Sizing up the nucleus: nuclear shape, size and nuclear-envelope assembly.* Journal of Cell Science, 2009. **122**(Pt 10): p. 1477-86.
110. Roukos, V., G. Pegoraro, T.C. Voss, and T. Misteli, *Cell cycle staging of individual cells by fluorescence microscopy.* Nature Protocols, 2015. **10**(2): p. 334-48.
111. Martin, H.L., M. Adams, J. Higgins, J. Bond, E.E. Morrison, S.M. Bell, S. Warriner, A. Nelson, and D.C. Tomlinson, *High-Content, High-Throughput Screening for the Identification of Cytotoxic Compounds Based on Cell Morphology and Cell Proliferation Markers.* Plos One, 2014. **9**(2).
*112.* Sun, X., T. Kovacs, Y.J. Hu, and W.X. Yang, *The role of actin and myosin during spermatogenesis.* Molecular Biology Reports, 2011. **38**(6): p. 3993-4001.
113. Kameoka, S., J. Babiarz, K. Kolaja, and E. Chiao, *A High-Throughput Screen for Teratogens Using Human Pluripotent Stem Cells.* Toxicological Sciences, 2014. **137**(1): p. 76-90.
114. Sirenko, O., T. Mitlo, J. Hesley, S. Luke, W. Owens, and E.F. Cromwell, *High-Content Assays for Characterizing the Viability and Morphology of 3D Cancer Spheroid Cultures.* Assay and Drug Development Technologies, 2015. **13**(7): p. 402-414.
115. Radio, N.M., J.M. Breier, T.J. Shafer, and W.R. Mundy, *Assessment of chemical effects on neurite outgrowth in PC12 cells using high content screening.* Toxicological Sciences, 2008. **105**(1): p. 106-118.
116. Anguissola, S., D. Garry, A. Salvati, P.J. O'Brien, and K.A. Dawson, *High Content Analysis Provides Mechanistic Insights on the Pathways of Toxicity Induced by Amine-Modified Polystyrene Nanoparticles.* Plos One, 2014. **9**(9).
117. Ramery, E. and P.J. O'Brien, *Evaluation of the Cytotoxicity of Organic Dust Components on THP1 Monocytes-Derived Macrophages Using High Content Analysis.* Environmental Toxicology, 2014. **29**(3): p. 310-319.
*118.* Versaevel, M., T. Grevesse, and S. Gabriele, *Spatial coordination between cell and nuclear shape*

*within micropatterned endothelial cells.* Nature Communications, 2012. **3**.
119. Persson, M., A.F. Loye, T. Mow, and J.J. Hornberg, *A high content screening assay to predict human drug-induced liver injury during drug discovery.* Journal of Pharmacological and Toxicological Methods, 2013. **68**(3): p. 302-313.
120. Dolinoy, D.C., D. Huang, and R.L. Jirtle, *Maternal nutrient supplementation counteracts bisphenol A-induced DNA hypomethylation in early development.* Proc Natl Acad Sci U S A, 2007. **104**(32): p. 13056-61.
121. Gassman, N.R., E. Coskun, P. Jaruga, M. Dizdaroglu, and S.H. Wilson, *Combined Effects of High-Dose Bisphenol A and Oxidizing Agent (KBrO) on Cellular Microenvironment, Gene Expression, and Chromatin Structure of Ku70-deficient Mouse Embryonic Fibroblasts.* Environ Health Perspect, 2016.
122. Jin, P., X. Wang, F. Chang, Y. Bai, Y. Li, R. Zhou, and L. Chen, *Low dose bisphenol A impairs spermatogenesis by suppressing reproductive hormone production and promoting germ cell apoptosis in adult rats.* Journal of Biomedical Research, 2013. **27**(2): p. 135-44.
123. Fisher, J.S., S. Macpherson, N. Marchetti, and R.M. Sharpe, *Human 'testicular dysgenesis syndrome': a possible model using in-utero exposure of the rat to dibutyl phthalate.* Human Reproduction, 2003. **18**(7): p. 1383-1394.
124. Kleymenova, E., C. Swanson, K. Boekelheide, and K.W. Gaido, *Exposure in utero to di(n-butyl) phthalate alters the vimentin cytoskeleton of fetal rat sertoli cells and disrupts sertoli cell-gonocyte contact.* Biology of Reproduction, 2005. **73**(3): p. 482-490.
125. Mahood, I.K., H.M. Scott, R. Brown, N. Hallmark, M. Walker, and R.M. Sharpe, *In utero exposure to di(n-butyl) phthalate and testicular dysgenesis: comparison of fetal and adult end points and their dose sensitivity.* Environ Health Perspect, 2007. **115 Suppl 1**: p. 55-61.
126. Saffarini, C.M., N.E. Heger, H. Yamasaki, T. Liu, S.J. Hall, and K. Boekelheide, *Induction and persistence of abnormal testicular germ cells following gestational exposure to di-(n-butyl) phthalate in p53-null mice.* J Androl, 2012. **33**(3): p. 505-13.
127. Ferrara, D., N. Hallmark, H. Scott, R. Brown, C. McKinnell, I.K. Mahood, and R.M. Sharpe, *Acute and long-term effects of in utero exposure of rats to di(n-butyl) phthalate on testicular germ cell development and proliferation.* Endocrinology, 2006. **147**(11): p. 5352-62.
128. Darzynkiewicz, Z., X. Huang, and M. Okafuji, *Detection of DNA strand breaks by flow and laser scanning cytometry in studies of apoptosis and cell proliferation (DNA replication).* Methods in Molecular Biology, 2006. **314**: p. 81-93.
129. Sidhu, J.S., R.A. Ponce, M.A. Vredevoogd, X.Z. Yu, E. Gribble, S.W. Hong, E. Schneider, and E.M. Faustman, *Cell cycle inhibition by sodium arsenite in primary embryonic rat midbrain neuroepithelial cells.* Toxicological Sciences, 2006. **89**(2): p. 475-484.
130. Liu, C., W. Duan, R. Li, S. Xu, L. Zhang, C. Chen, M. He, Y. Lu, H. Wu, H. Pi, X. Luo, Y. Zhang, M. Zhong, Z. Yu, and Z. Zhou, *Exposure to bisphenol A disrupts meiotic progression during spermatogenesis in adult rats through estrogen-like activity.* Cell Death & Disease, 2013.**4**.
131. Ali, S., G. Steinmetz, G. Montillet, M.H. Perrard, A. Loundou, P. Durand, M.R. Guichaoua, and O. Prat, *Exposure to low-dose bisphenol A impairs meiosis in the rat seminiferous tubule culture model: a physiotoxicogenomic approach.* PLoS One, 2014. **9**(9): p. e106245.
132. Bouskine, A., M. Nebout, F. Brucker-Davis, M. Benahmed, and P. Fenichel, *Low Doses of Bisphenol A Promote Human Seminoma Cell Proliferation by Activating PKA and PKG via a Membrane G-Protein-Coupled Estrogen Receptor.* Environmental Health Perspectives, 2009. **117**(7): p. 1053-1058.
133. Pfeifer, D., Y.M. Chung, and M.C.T. Hu, *Effects of Low-Dose Bisphenol A on DNA Damage and Proliferation of Breast Cells: The Role of c-Myc.* Environmental Health Perspectives, 2015. **123**(12): p. 1271-1279.
134. Wu, S., X.T. Wei, J.J. Jiang, L.Q. Shang, and W.D. Hao, *Effects of bisphenol A on the proliferation and cell cycle of HBL-100 cells.* Food and Chemical Toxicology, 2012. **50**(9): p. 3100-3105.
135. Keri, R.A., S.M. Ho, P.A. Hunt, K.E. Knudsen, A.M. Soto, and G.S. Prins, *An evaluation of evidence for the carcinogenic activity of bisphenol A.* Reproductive Toxicology, 2007. **24**(2): p. 240-252.
136. Marchetti, C., S.A. Walker, F. Odreman, A. Vindigni, A.J. Doherty, and P. Jeggo, *Identification of a novel motif in DNA ligases exemplified by DNA ligase IV.* DNA Repair (Amst), 2006. **5**(7): p. 788-98.
*137.* Rogakou, E.P., D.R. Pilch, A.H. Orr, V.S. Ivanova, and W.M. Bonner, *DNA double-stranded breaks*

*induce histone H2AX phosphorylation on serine 139.* Journal of Biological Chemistry, 1998. **273**(10): p. 5858-5868.

138. Nikolova, T., M. Dvorak, F. Jung, I. Adam, E. Kramer, A. Gerhold-Ay, and B. Kaina, *The gamma H2AX Assay for Genotoxic and Nongenotoxic Agents: Comparison of H2AX Phosphorylation with Cell Death Response.* Toxicological Sciences, 2014. **140**(1): p. 103-117.
139. Fic, A., B. Zegura, M.S. Dolenc, M. Filipic, and L.P. Masic, *Mutagenicity and DNA Damage of Bisphenol a and Its Structural Analogues in Hepg2 Cells.* Archives of Industrial Hygiene and Toxicology, 2013. **64**(2): p. 189-200.
140. Lee, S., X. Liu, S. Takeda, and K. Choi, *Genotoxic potentials and related mechanisms of bisphenol A and other bisphenol compounds: A comparison study employing chicken DT40 cells.* Chemosphere, 2013. **93**(2): p. 434-440.
141. Audebert, M., L. Dolo, E. Perdu, J.P. Cravedi, and D. Zalko, *Use of the gamma H2AX assay for assessing the genotoxicity of bisphenol A and bisphenol F in human cell lines.* Archives of Toxicology, 2011. **85**(11): p. 1463-1473.
142. Lie, P.P.Y., D.D. Mruk, W.M. Lee, and C.Y. Cheng, *Epidermal growth factor receptor pathway substrate 8 (Eps8) is a novel regulator of cell adhesion and the blood-testis barrier integrity in the seminiferous epithelium.* Faseb Journal, 2009. **23**(8): p. 2555-2567.
143. Xiao, X., D.D. Mruk, E.I. Tang, C.K.C. Wong, W.M. Lee, C.M. John, P.J. Turek, B. Silvestrini, and C.Y. Cheng, *Environmental toxicants perturb human Sertoli cell adhesive function via changes in F-actin organization mediated by actin regulatory proteins.* Human Reproduction, 2014. **29**(6): p. 1279-1291.
144. Zhao, X.X., T. Toyooka, T. Kubota, G. Yang, and Y. Ibuki, *gamma-H2AX induced by linear alkylbenzene sulfonates is due to deoxyribonuclease-1 translocation to the nucleus via actin disruption.* Mutation Research-Fundamental and Molecular Mechanisms of Mutagenesis, 2015. **777**: p. 33-42.
145. Lei, B., J. Xu, W. Peng, Y. Wen, X. Zeng, Z. Yu, Y. Wang, and T. Chen, *In vitro profiling of toxicity and endocrine disrupting effects of bisphenol analogues by employing MCF-7 cells and two-hybrid yeast bioassay.* Environmental Science & Technology, 2016.
146. Roelofs, M.J.E., M. van den Berg, T.F.H. Bovee, A.H. Piersma, and M.B.M. van Duursen, *Structural bisphenol analogues differentially target steroidogenesis in murine MA-10 Leydig cells as well as the glucocorticoid receptor.* Toxicology, 2015. **329**: p. 10-20.
147. Eladak, S., T. Grisin, D. Moison, M.J. Guerquin, T. N'Tumba-Byn, S. Pozzi-Gaudin, A. Benachi, G. Livera, V. Rouiller-Fabre, and R. Habert, *A new chapter in the bisphenol A story: bisphenol S and bisphenol F are not safe alternatives to this compound.* Fertility and Sterility, 2015. **103**(1): p. 11-21.
148. D'Cruz, S.C., R. Jubendradass, M. Jayakanthan, S.J.A. Rani, and P.P. Mathur, *Bisphenol A impairs insulin signaling and glucose homeostasis and decreases steroidogenesis in rat testis: An in vivo and in silico study.* Food and Chemical Toxicology, 2012. **50**(3-4): p. 1124-1133.
149. Tiwari, D. and G. Vanage, *Mutagenic effect of Bisphenol A on adult rat male germ cells and their fertility.* Reproductive Toxicology, 2013. **40**: p. 60-8.
150. Feng, Y.X., J. Yin, Z.H. Jiao, J.C. Shi, M. Li, and B. Shao, *Bisphenol AF may cause testosterone reduction by directly affecting testis function in adult male rats.* Toxicology Letters, 2012. **211**(2): p. 201-209.
151. Kuriyama, S.N., C.E. Talsness, K. Grote, and I. Chahoud, *Developmental exposure to low-dose PBDE-99: Effects on male fertility and neurobehavior in rat offspring.* Environmental Health Perspectives, 2005. **113**(2): p. 149-154.
152. Ullah, H., S. Jahan, Q.U. Ain, G. Shaheen, and N. Ahsan, *Effect of bisphenol S exposure on male reproductive system of rats: A histological and biochemical study.* Chemosphere, 2016. **152**: p. 383-9.